NATIONAL ADVISORY COMMITTEE FOR AERONAUTICS

TECHNICAL MEMORANDUM

No. 1112

THE EFFECT OF TURBULENCE ON THE FLAME VELOCITY IN GAS MIXTURES

By Gerhard Damköhler

Zeitschrift für Elektrochemie und angewandte
Physikalische Chemie. Vol. 46, No. 11, Nov. 1940

Washington
April 1947

NATIONAL ADVISORY COMMITTEE FOR AERONAUTICS

TECHNICAL MEMORANDUM NO. 1112

THE EFFECT OF TURBULENCE ON THE FLAME VELOCITY IN GAS MIXTURES[1]

By Gerhard Damköhler

The present report deals with the effect of turbulence on the propagation of the flame. Being based upon experiments with laminar as well as turbulent Bunsen flames, both the physico-chemical and the hydrodynamical aspects of the problem are analyzed.

A number of new deductions, interesting from the point of view of engine combustion and other very rapidly changing flame reactions, are made.

SUMMARY

1. By use of the Bunsen burner method on various propane-oxygen mixtures, a number of flame velocity measurements were made in the range of Reynolds numbers Re = 612 to 17300 (referred to inside diameter of burner tube), so that the appearance of the turbulent Bunsen flame could be compared with that of the laminar. The inside diameters d of the employed tubes I, II, and III were 1.385, 2.18, and 2.718 millimeters, respectively.

2. The laminar Bunsen flame burned completely without noise. It showed a sharply defined bell-shape flame surface, the base of which extended a little over the inside cross section of the burner tube. The tip of the cone was rounded off with a curvature radius of the same order of magnitude as the luminous thickness δ_L of the flame surface itself; the thickness of the luminous zone δ_L was measured from time to time just a little below the cone tip and amounted to 0.10 ±0.02 millimeter in all the laminar tests.

3. The turbulent flame was recognized acoustically by loud whistling. The zone of the flame, which in its base, also extended over the internal cross section of the burner tube, was no longer sharply defined, but

---

[1] "Der Einfluss der Turbulenz auf die Flammengeschwindigkeit in Gasgemischen." Zeitschrift für Elektrochemie und angewandte Physikalische Chemie. Vol. 46, no. 11, Nov. 1940, pp. 601 - 626.

washed out. The zones were no longer bell-shape except on the narrowest tube I; they were already rather bolt-shape on the wider tube II, and on tube III its upper part was considerably enlarged with respect to its base.

4. From the boundary surfaces of the turbulent flame zone, even though blurred, the existing maximum and minimum flame velocities, $\bar{w}_{f\,max}$ and $\bar{w}_{f\,min}$, can be approximately computed.

With exception of two tests the minimum flame speeds $\bar{w}_{f\,min}$ agreed consistently with the corresponding flame speed $\bar{w}_{fl}$ for laminar flow. The two unsuccessful tests can, however, be interpreted likewise.

At small Reynolds numbers the ratio $\frac{\bar{w}_{f\,max}}{\bar{w}_{f\,min}}$ increases (tube I and II with Re = 2300 to 5000) approximately proportionally to $\sqrt{Re}$ at large Reynolds numbers (tubes II and III with Re = 5000 to 18000) approximately linearly with Re.

5. The theory of laminar, stationary flame zone is briefly discussed. The terms "preparation zone", "reaction zone", "ignition temperature", "rate of chemical reaction", and "flame speed," are explained and the mathematical relations existing between these quantities deduced. Numerical values for the quantities are given on the basis of the experimental material.

6. The mean chemical decomposition velocity in the reaction zone amounts to about 0.2 mol of fuel per cubic centimeter times seconds in the tests, so that every fuel molecule receives approximately 10^5 impulses before being completely burned.

7. Comparison of the computed thicknesses of the preparation and reaction zones, δ_V and δ_R, respectively, with the experimentally established luminous zone thickness δ_L, gives the fairly arbitrary alternative: the ignition temperature $\vartheta_Z \approx 500^\circ$ C in the flame either agrees approximately with the autoignition temperatures determined for the particular mixture by the method of adiabatic compression or with the Dixon burner arrangement; in which case $\delta_L \approx \delta_V + \delta_R$; or else with $\vartheta_Z \approx 200^\circ$ C the ignition temperature in the flame lies considerably lower than the cited autoignition temperatures; in which case $\delta_L \approx \delta_R$. The second possibility appears more likely at the present time. Investigation of the intensity distribution of the individual emission spectrums in δ_L would also afford insight into the time sequence of its occurrence and thus contribute considerably to the elucidation of the chemical reaction mechanism in the flame.

8. The propagation of a laminar free jet is numerically estimated after an article by H. Schlichting and found to be compeletely negligible for the interpretation of the laminar Bunsen cone. However, the experimentally observed laminar flame cones do not completely agree in form with cones computable on the assumption of a parabolic velocity profile and equal flame speed at every point of the flame cone. The discrepancies can be explained. Directly above the burner tube rim a horizontal, outwardly directed flow must exist, which can be numerically appraised, and which effectively prevents air from the outside being diffused into the cone of the flame.

9. Prandtl's characterization of the turbulence of a flow by two numerical quantities is briefly outlined: by the mixing length l, which indicates the approximate magnitude of the turbulence bodies, and by the exchange quantity e, which, as a type of diffusion coefficient, permits a quantitative statement concerning the amplified transport processes in turbulent flow. With these two quantities the turbulence in the free jet issuing from a tube orifice is numerically estimated, it itself being divided into a nuclear zone with the flow and turbulence properties as in a simple pipe (explored by Nikuradse) and a border zone with particular characteristics (investigated by W. Tollmien).

10. The theoretically conceivable influences of the turbulence on the propagation of flames are discussed. Two types of turbulence with totally different effects must be distinguished: "coarse-body turbulence with a great mixing length compared to the thickness of the laminar combustion zone, with roughened and ultimately scattered flame front, in which, as a result, the surface of the flame is enlarged, and the flame speed referred to the flow cross section rises beyond the laminar value w_{fl}. On the extremely "fine-body" turbulence with very short mixing length compared to laminar flame zone thickness, there is no roughening of flame surface. On the other hand, all transport processes in it are greater; hence also the rise in turbulent flame speed w_{ft} beyond the laminar w_{fl}, which is, according to the formula,

$$\frac{w_{ft}}{w_{fl}} = \sqrt{\frac{\epsilon}{\nu}}$$

The values of $\overline{w}_{ft}$ computed with it (averaged over the total flow cross section) are only about 30 percent higher than the experimentally established maximum flame speeds in the turbulent flame. Hence in the tests, besides the rough-body turbulence, the fine-body turbulence also must have played a part; especially since the greatest mixing lengths in the three burner tubes amounted to 0.11, 0.17, and 0.21 millimeter respectively, while the luminous zone thickness was fixed at $\delta_L = 0.1$ millimeter.

For the combustion in the Otto-cycle engine the coarse-body turbulence is likely to be decisive, although its effect is as yet unpredictable; because turbulence bodies of the order of $l = 0.1$ millimeter can be produced only for gas issuing from very narrow flow cross sections, and such are always to be avoided for reasons of the high flow resistances involved.

11. In turbulent interchange or mixing processes it is always necessary to distinguish between transport lengths that are greater or smaller than the mixing length l. In the latter case the Prandtl interchange quantity is effective only with a fractional amount of its macroscopic value e.

INTRODUCTION

The earlier reports on flame speed (ignition velocity) in gas mixtures deal exclusively with the propagation of flames in static or laminar gas flow (in the bomb, in the pipe closed at both ends, in the soap bubble, or in the Bunsen burner, etc). The reports further define the physical and chemical influences (pressure, initial temperature, type of container walls, chemical composition of initial gas) and attempt to explain the phenomenon of flame propagation theoretically and from it deduce physical and kinetic reaction data.

But not one of these reports contains any information about the propagation of flames in turbulent gas flow, although this case is of considerable importance for the technique. In the Otto-cycle engine, for instance, flame speeds of from 10 to 50 meters per second occur, which are due solely to turbulence effect (measured relative to cylinder head), that is, from 10 to 100 times the amount of the value measured on the same gas mixture without turbulence. However, it still remains to be explained whether these high combustion speeds in the engine are simulated by gas masses that flow faster than they burn or whether really higher flame speeds are involved, the cause of which might be found in the turbulent motion, but likely also in dynamic gas effects.

The little knowledge of the influence of pure turbulence on the flame speed may be due to the following causes: in the first place it is difficult to identify the turbulence of a flow quantitatively. So far this has been successfully accomplished only for the developed turbulence in stationary flow. (Cf. the fundamental works by L. Prandtl and his school as well as the more recent British and American wind-tunnel investigations on the subject.) On top of that these reports are scarcely known to engineers and physico-chemists interested in the problem of flame speed.

The subsequent report is a first attempt to measure exactly the influence of turbulence on flame propagation and to interpret it theoretically. To this end comparable flame speed measurements were made in laminar and fully developed turbulent flow on various uniformly flowing gas mixtures. It is true that the latter case corresponds only in part to the conditions encountered in the Otto engine, but it also makes it possible to give numerical data on the state of turbulence of the flow which are indispensible for a deeper insight into the processes involved.

The theoretical treatment of the experimental data begins with the development of the general theory of the stationary flame zone in laminar flow; then follow the numerical data on preparation zone, reaction zone, ignition temperature, and chemical reaction speed in the cone of the laminar Bunsen burner, the enlargement of a laminar gas jet issuing into the open and the form of Bunsen cone burning in it, quantitative appraisal of the conditions of turbulence in the free jet in the light of the Prandtl school, discussion of the theoretically conceivable turbulence effects on the flame speed, and lastly, comparison with the test data of the present study.

TEST METHOD AND TEST DATA

1. Principles

The measurement of the effect of turbulence on flame propagation in a flowing gas mixture is predicated upon the numerical data on the turbulence.

The only method of flame speed measurement in which definite and well-known flow conditions exist and in which wall effects are also excluded as far as possible, is the Bunsen burner method. Here a flame cone stands stationary in an open jet that issues from a burner tube and in its core still manifests the same turbulence as the flow in the tube. Very carefully executed measurements of turbulence in pipe flow are available (reference 1); while the turbulence in the boundary zone of the free jet, as investigated mathematically by W. Tollmien (reference 2), showed good agreement with Gottingen wind-tunnel measurements. Through these studies the turbulence in the free jet is known.

Admittedly, the simple burner tube has the drawback of a locally dependent flow velocity and turbulence, hence necessitates integration over the entire flow cross section. But then the turbulence is known and need not be measured first.

2. Experimental Setup

The setup, is diagrammatically shown in figure 1. The gases from storage tanks A_1 and A_2 pass, at first, separately across the bubble valves B_1 and B_2 (with controlled immersion depth) filled with water or mercury, depending upon the flow velocities, into the calibrated flow meters st_1 and st_2. From there they pass across the pressure-equalizing flasks D_1 and D_2 and the reducing valves V_1 and V_2 into the mixing piece T, topped by the actual burner tube B. Pressure fluctuations were avoided by the control of valves V_1 and V_2 in conjunction with flasks D_1 and D_2; hence the flame burned perfectly still. A glass tube R (80 mm in diameter, 300 mm long) slipped over the burner provided protection against draft. The dimensions of the brass burner tubes are given in table 1.

TABLE 1

DIMENSIONS OF BURNER TUBES

Tube	Length	Diameter (mm)		Wall thickness at mouth	$\frac{L}{d}$
		Outside	Inside		
I	500	2.0	1.385	0.30	361
II	500	4.0	2.18	.11	229
III	1000	5.0	2.718	.60	368

Tubes I and II were tapered at the upper end over a 20-millimeter length so that the outside diameters and hence the wall thicknesses decreased to the figures cited in the table. The relative entrance lengths $\frac{L}{d}$ exceed the value of 150 and 50 necessary to produce developed flow several times over in laminar flow (reference 3) as well as in turbulent flow (reference 1). These lengths were intentionally chosen greater in order to ensure complete mixing of the gases, which was further aided by the T piece. In the preliminary tests the flame cones necessary for the calculation of the flame speed were measured direct with the small telescope of a cathetometer, in the principal tests by photographic recording and subsequent measuring of the positive prints. A scale near the burner orifice (fig. 1) was also photographed (1 division = 1/2 mm). After considerable trials the Afga-Kontrast plate 6.5 × 9 square centimeters proved the most suitable.

3. Experimental Gases

The gases consisted of various blends of technical oxygen and technical propane, which is essentially a propane–butane mixture, containing about 6 percent of unsaturated hydrocarbons (olefins). It might be suspected that more rapid vaporization of the easier boiling propane in the original steel flask would gradually enrich the rest of the butane; but this was not the case as proved by several molar weight determinations[1], which, while manifesting fluctuations, indicated no systematic time process. It is likely that the inferior diffusion coefficient of the fluid propane–butane mixture provided for practically total vaporization on the surface of the liquid. The mean mole weight of propane in the tests was $M = 46.1 \pm 0.5$ corresponding to a propane content of 85 ± 5 percent, if the rest is regarded as butane.

The Reynolds number in the burner tube was computed by means of the viscosity of the gas mixtures with the apparatus shown in figure 2. It consisted largely of a glass tube spiral of about 1-millimeter inside diameter. The entrance length AB was about 500 millimeters, the actual test length BC, 1000 millimeters. The flow is laminar at Reynolds numbers ranging between 100 and 500, hence the following relation for pressure drop between B and C:

$$\Delta p = k \eta G$$

where

η dynamic viscosity

G flow volume

k constant

The latter was empirically determined by calibration measurements with pure oxygen at $47 \times 13 \times 10^4$, with $\eta_{O_2} = 2.05^0 \times 10^{-4}$ grams per centimeter^{-1} second^{-1}.

The recorded viscosities are reproduced in table 2 and figure 3; they were all made at $18 \pm 1^\circ$ C with a propane of density 1.92×10^{-3} grams per cubic centimeter ($M = 45.9$).

4. Experimental Results

The subsequent data refer almost exclusively to the principal tests, because in the preliminary tests in which the flame cones were

---

[1]With the Kahle type gas sweep obtained from Linde's Eismaschinen (Hollriegelskreuth, near Munich).

measured visually with cathetometer, the extent of dispersion of the observed flame velocities amounted to 20 percent, as against less than ± 10 percent on the averaged main test curves (fig. 5). Particularly uncertain in the preliminary tests was the gaging of the blurred turbulent flame zones, since the field of vision of the small telescope covered only part of the flame; whereas the positive print of the photographs in the principal tests always presented the entire flame and made it much easier to identify individual zones. These zones were then outlined by pencil and measured with the telescope of the cathetometer. The photographs of the individual flames are reproduced in figure 4 and tabulated in table 3. The flame phenomena obtained were distinctly different, depending upon whether the flow in the burner tube was laminar or turbulent.

The laminar flow ($Re << 2300$) burnt absolutely without noise. It revealed a sharply defined bell-shape flame surface, the base of which extended over the internal cross section of the burner tube. The tip of the cone was rounded off with a curvature radius of the same order of magnitude as the thickness of the luminous flame surface. This luminous cone thickness was measured from time to time just a little below the tip of the cone and ranged between 0.10 ± 0.02 millimeter throughout all laminar tests.

The turbulent flame ($Re >> 2300$) was accompanied by a loud whistle. The zone of flame, which in its base also extended over the internal cross section of the burner tube, was no longer sharply defined but blurred. Only the narrowest tube I disclosed a bell-shape form; on tube II it became bolt-shape and on tube III the upper part was already considerably wider than at the base.

For the quantitative interpretation of the test data the flame velocity w_f (cm/sec) averaged over the flame cone was calculated; it indicates the speed at which the flame burns against the stationary gas flow. According to Gouy the following relation (reference 4) is applicable:

$$w_f = G/F \qquad (1)$$

where

G amount of gas supplied to burner, cubic centimeters per second

F surface of flame cone, square centimeters

With F computed as the surface of a body of rotation by Passus' theorem $F = 2\pi R'S$ from the length S of the enveloping line of the combustion cone outlined by pencil and the distance R' of its center of gravity from the center line, the outer or inner boundary surface of the flame zone can be used as a basis. The former served in the preliminary tests because it was easier to measure by the visual observation of the flame, while in the principal tests one flame

velocity each was determined for both luminous zone boundaries, the intention being to evaluate laminar and turbulent tests as nearly alike as possible. Closer examination of figure 4, especially the comparison of photographs 49 and 50 with 51 and 53 reveals that the turbulent flame zone issues from the laminar in such a manner that the boundary surfaces of the laminar luminous zone shift farther apart and at the same time become hazy. But in the turbulent flame these fairly distant and, in addition, blurred boundary surfaces are the only definite areas that can be measured and both of them must therefore be considered if a somewhat quantitative picture of the total flame phenomenon is to be secured.

Both boundaries have, moreover, a physical significance also; the inner is the locus of the speediest combustion, the outer, of the slowest combustion. The slowest flame velocities of the turbulent flame for all three tubes agreed with the flame velocity for laminar flow (identical mixture presumed) according to table 3 and figure 5. This result is very obvious; for a flame velocity slower than for laminar flow can be visualized only when the initial gas, before its complete combustion is diluted by incombustible gas additions (for instance, products of combustion), which would be conceivable in the upper parts of a flame for strongly turbulent mixing motion. This condition probably takes part in tests 52 and 45 which alone fell out of line. Possibly the "marginal turbulence" of the free jet exerts here such a delaying effect. In test 52 $\bar{w}_{f\ min}$ is smaller than the corresponding laminar flame velocity (cf. fig. 5) and test 45 disclosed an irregularity in the ratio $\frac{\bar{w}_{f\ max}}{\bar{w}_{f\ min}}$ (cf. fig. 6).

So, since the ratio $\frac{\bar{w}_{f\ max}}{\bar{w}_{f\ min}}$ is a measure for the increase in flame velocity due to turbulence, it was plotted in figure 6(a) and 6(b) against the Reynolds number $Re = \frac{\bar{u}d}{\nu}$ of the tube flow and against $\sqrt{Re}$. The graphs show: for $2300 < Re < 5000$ (1.385 and 2.18 mm tube diameter), $\frac{\bar{w}_{f\ max}}{\bar{w}_{f\ min}}$ increases approximately proportionately to $\sqrt{Re}$, for $5000 < Re < 18000$ (tube diameters 2.18 and 2.78 mm) approximately linearly with Re. For the present, these experimentally obtained relations should be regarded as approximate formulas, because of the marked scattering of the test points.

Lastly, it may be mentioned that when using a burner tube of only 500-millimeter length and 2.718-millimeter diameter, hence with a relative entrance length $L/d = 184$, the outer boundary of the turbulent flame zone revealed from time to time single, plainly distinguishable gas bodies, which burned by themselves. But this phenomenon was not repeated on the twice-as-long tube III. Therefore the entrance length

of the 500-millimeter tube was apparently insufficient for complete mixture of the original gases.

III. THEORY - DISCUSSION OF TEST DATA

1. Theory of Stationary Flame in Laminar Flow

The flame front is divided into a preparatory zone (in the literature usually termed "preheating zone") (reference 5) and a reaction zone. At the boundary surface of these two zones the ignition temperature ϑ_z prevails. This demarcation is also useful as approximation for the modern conception of the combustion processes; for these always have, as chain reactions, a certain induction period, during which the mixture, by forming or diffusion of active intermediate products as well as by heat input, must first be prepared for ignition. Here the entire chemical decomposition remains at first quite small, usually less than 1 percent. At the place of the ignition temperature ϑ_z the concentrations of the active chain carriers and the reaction velocities of the individual elementary reactions have by then become so great that the total decomposition velocity suddenly speeds up: here the reaction zone starts.

Only in one respect do the modern conceptions show an essential difference from the earlier ones: the ignition temperature may not be regarded as a characteristic physical constant of the initial mixture, as pointed out by Jost and Von Muffling (reference 6). Neither can the ignition temperature ϑ_z occurring in the flame on the border between preparatory zone and reaction zone be expected to agree with the ignition temperatures that are obtained for the same initial mixture by the Nernst method of adiabatic compression or Dixon's burner tube. It is likely that the ignition temperature ϑ_z in the flame is lower, because ignition takes place under more favorable conditions than in the other two cases, in which the intermediate products necessary for ignition must be formed purely thermally. In the preparatory zone of the flame, on the other hand, these substances are supplied by diffusion from the reaction zone. Thus the new thermal formation of active substances can be smaller or be absent altogether. That the diffusion flow of these active intermediate products against the actual gas flow is substantial, has been demonstrated by Jost and Von Muffling.

The conditions in the flame front in stationary flow are defined by the following equation system (reference 7). Conservation of momentum:

$$\rho(\underline{w}\,\nabla)\,\underline{w} = -\nabla p + \eta\left[\Delta\,\underline{w} + \frac{1}{3}\,\text{grad div}\,\underline{w}\right] \qquad (2)$$

Conservation of energy:

$$0 = QU - \operatorname{div}\,(c_p \rho \underline{w} \vartheta \quad \operatorname{div}\,(-\lambda\,\operatorname{grad}\vartheta) \tag{3}$$

Conservation of atom type:

$$0 = -\nu_j U - \operatorname{div}\,(n_j \underline{w}) - \operatorname{div}\,(-D_j \operatorname{grad} n_j) \tag{4}$$

where:

$\underline{w}$ flow velocity

ρ density

p pressure

ϑ temperature

c_p specific heat of mixture

η dynamic viscosity

λ thermal conductivity

Q heat of reaction

U chemical reaction speed (mol/cm^3 sec)

n_j number of mols of the particle type j per unit of volume

ν_j stoichiometric conversion factor

D_j diffusion coefficient of the particle type j

The solution requires the integration in the preparatory zone with $U = 0$ and in the reaction zone with $U \neq 0$.

Assuming the same total pressure at all points (which holds good accurately enough in the slow combustion of normal flames, but not in detonation processes, of course) and limited to one-dimensional flow, equation (2) cancels and $\underline{w}$ is simply defined by the equation of continuity

$$\rho \underline{w} = \text{constant} = \rho_a \underline{w}_a \tag{5}$$

subscript a denoting the initial state.

Lastly, there is the equation defining the laminar flame velocity

$$w_{fl} = |w_a| \tag{6}$$

Integration of equation (3) over the preparatory zone (U = 0) between the initial state at $x = -\infty$ and the point of ignition (subscript z) at $x = 0$, where $\lambda \frac{\partial \vartheta}{\partial x} = 0$ for $x = -\infty$, gives

$$\bar{c}_p \rho_a w_a (\vartheta_z - \vartheta_a) = \lambda_z \left(\frac{\partial \vartheta}{\partial x} \right)_z \tag{7}$$

with c_p denoting the mean specific heat of flowing gas between ϑ_a and ϑ_z. Assuming the thermal conductivity in the preparatory zone as being constant, or computing with a suitable average value $\lambda = \bar{\lambda}$, the integration of equation (3) gives the temperature variation in the preparatory zone:

$$\vartheta - \vartheta_a = (\vartheta_z - \vartheta_a) \; e^{\frac{\bar{c}_p \rho_a w_a x}{\bar{\lambda}}} \tag{8}$$

(also given in reference 4, p. 20). From this a thickness of the preparatory zone $\delta_v = -x$ can be estimated when assuming for this x, for example: $\frac{\vartheta - \vartheta_a}{\vartheta_z - \vartheta_a} = \frac{1}{100}$.

It then yields

$$-2 = \frac{\bar{c}_p \rho_a w_a (-\delta_v)}{\bar{\lambda}} \lg^{10} e \tag{9}$$

or, with allowance for equation (6):

$$\delta_v \approx \frac{5\bar{\lambda}}{\bar{c}_p \rho_a w_{fl}} \tag{10}$$

The thickness of the preparatory zone is thus reduced to the determination of the laminar flame velocity w_{fl}. Unfortunately it has not been possible up to now to check the thus computed values of δ_v by actual experiment. But they will be useful for the understanding of the turbulence effect on the flame velocity.

An integration of equation (4) (there is one equation each for each type of molecule) over the preparatory zone would result in relations similar to equation (7), except for the concentrations n_j substituting for temperature ϑ and the diffusion coefficients D_j replacing the thermal conductivity λ. Several additional assumptions would even afford equations corresponding to equation (8), and which

would describe the penetration of the active intermediate products from the reaction zone into the preparatory zone, so far as a new thermal formation of these intermediate products in the preparatory zone itself can be excluded.

Important for the subsequent study is the integration of that equation (4) which refers to the fuel particle itself (subscript b instead of j), the integrations being directly extended to cover the entire flame zone, or preparatory zone + reaction zone. Now, if the stoichiometric conversion factor for the fuel particle is standardized to $\nu_b = 1$, that is, if U indicates the number of mols of fuel per volume per unit time converted at a point of the reaction zone (with $U = 0$ in the preparatory zone as before), and it is borne in mind that at both limits $x = -\alpha(x \sim -\delta_V$, respectively), and $x = \delta_R$ (end of reaction zone) the expressions $D_b \frac{\partial n_b}{\partial x}$ disappear, and further that $n_b = n_{ba}$ at start and $n_b = 0$ at finish,

$$n_{ba}\, w_a = \int_{-\infty}^{\delta_R} U\, dx = \int_{0}^{\delta_R} U\, dx = \bar{U} \times \delta_R \qquad (11)$$

or with equation (6):

$$n_{ba}\, w_{fl} = U\, \delta_R \qquad (12)$$

$\bar{U}$ represents the mean chemical reaction speed (mol/cm^3 sec fuel) in the reaction zone. Hence $\bar{U}$ is directly linked with the thickness of the reaction zone δ_R and the laminar ignition velocity w_{fl}. Naturally, equation (12) could also have been posted immediately for continuity reasons, but this method affords a better picture of the physical view points that play a part in the solution of the complicated system of equations (3) and (4) by approximation. In the preparatory zone it was the temperature rise[1]; in the reaction zone it was the disappearance of the fuel with a mean chemical conversion speed U.

The relation ensuring the continuous connection between reaction zone and preparatory zone is obtained as follows: putting, similar to A. Eucken (reference 8)

$$\left(\frac{\partial \vartheta}{\partial x}\right)_z = \frac{\vartheta_e - \vartheta_z}{\delta_R}\, f \qquad (13)$$

---

[1]For which reason the earlier reports always spoke only of the preheating zone, whereas the term "preparatory zone" fits the nature of the phenomenon much better.

f signifying, for the time being, an open numerical factor, but which cannot be overly far from unity, and ϑ_e denoting the terminal combustion temperature. This becomes apparent on the actual temperature curve in the flame zone, which is plotted to scale in figure 7(a) and 7(b) on the basis of subsequently computed numerical values. From (6), (7) and (13) the thickness of the reaction zone follows

$$\delta_R = \frac{f \times \lambda_z (\vartheta_e - \vartheta_z)}{c_p \rho_a w_{fl} (\vartheta_z - \vartheta_a)} \tag{14}$$

Elimination of δ_R from (12) and (14) leaves essentially a relation between flame velocity w_{fl}, thermal conductivity λ_z and mean chemical reaction speed $\bar{U}$:

$$w_{fl}^2 = \frac{f \lambda_z \bar{U} (\vartheta_e - \vartheta_z)}{c_p \rho_a n_{ba} (\vartheta_z - \vartheta_a)} \tag{15}$$

Naturally, equation (15) can also be solved with respect to $\bar{U}$; hence $\bar{U}$ in the laminar flame can be obtained from experimentally accessible quantities. This will be done later, at which time it will also be considered whether $\bar{U}$ in the normal flame is actually so small that - from the pure kinetic reaction point of view - still substantially higher $\bar{U}$ values can be visualized, which should appear then, for example, in detonation processes.

Formula (15) is essentially agreeable with the relations of Jouget, Nusselt and Daniel, but rather than assume a special law for the chemical reaction speed U, the factor f is introduced.

2. Numerical Values for Preparatory Zone, Reaction Zone, Ignition Temperature and Chemical Reaction Speed in the Cone of the Laminar Bunsen Flame

The data for a mixture of 15 percent propane and 85 percent oxygen are according to the foregoing test data and the literature, respectively, as follows:

molal weight: $M = 34.1$

density: $\rho_a = 1.52 \times 10^{-3}$ g cm^{-3} at N.T.P. (=760 mm Hg, and 0° C)

initial concentration: $n_{ba} = 6.7 \times 10^{-6}$ mol/cm³ fuel N.T.P.

flame velocity: w_{fl} = (300 ± 30)cm/sec) at N.T.P.

initial temperature: $\vartheta_a = 0^\circ$ C

terminal temperature: $\vartheta_e = 3000^\circ$ C (hypothetical value)

ignition temperature: $\vartheta_z = 500^\circ$ C and 200° C, respectively

mean temperature in preparatory zone: $\bar{\vartheta} = 250^\circ$ C and 100° C, respectively

Since it was not possible to make any predictions about the actual amount, beforehand, two ignition temperatures were tentatively assumed. The specific heats $\bar{c}_p$ were additively computed from the mol heats C_p of the single gases. The assumed values are contained in table 4, in which the limit of error of the propane values was intentionally put very high:

TABLE 4

ϑ° C	$C_p O_2$ (reference 9) cal/mol grad	C_p propane[1] cal/mol grad	C_p mixture cal/mol grad
100	7.15	16.4 ± 3.0	8.54 ± 0.45
250	7.50	24.8 ± 4.0	10.1 ± 0.60

Hence for $c_p = \dfrac{C_{p\ \text{mixture}}}{34.1}$ the numerical values

at $\bar{\vartheta} = 100^\circ$ C: $\bar{c}_p = 0.25 \pm 0.01$ cal g^{-1} $grad^{-1}$

$\bar{\vartheta} = 250^\circ$ C: $\bar{c}_p = 0.30 \pm 0.02$ cal g^{-1} $grad^{-1}$

The thermal conductivities of the mixture were computed additively from the values for the pure components by means of the following

[1]Chemical Ing. vol. III, 1 p. 102 gives for 327° C for CH_4, C_2H_6 and n-C_5 H_{10} the mol/heats C_p = 12.61 -> 20.98 -> 38.0, hence the value 29 ± 5 for propane at the same temperature is entirely plausible. For 0° C the propane value was assumed at C_p = 14 ± 3. The C_p values for temperatures between 0° C and 327° C are linearly interpolated.

numerical values (λ in kcal m^{-1} h^{-1} grd^{-1}), the limit of error being again made very wide.

TABLE 5

ϑ °C	λ O_2	λ propane[1]	λ mixture
100	0.027	0.027 ± 0.003	0.027 ± 0.000
200	.031	.040 ± .015	.032 ± .002
250	.033	.047 ± .020	.035 ± .003
500	.044 ± .006[2]	.80 ± .040	.049 ± .010

Hence for λ in c.g.s. units:

$\vartheta_z = 500^\circ$ C $\lambda_z = (136 \pm 28) \times 10^{-6}$ cal cm^{-1} sec^{-1} $grad^{-1}$

$\bar{\vartheta} = 250^\circ$ $\bar{\lambda} = (97 \pm 9) \times 10^{-6}$

$\vartheta_z = 200^\circ$ $\lambda_z = (89 \pm 6) \times 10^{-6}$

$\bar{\vartheta} = 100^\circ$ $\bar{\lambda} = (75 \pm 2) \times 10^{-6}$

[4]From equation (10), (7), (12), and (14) then follow for the two assumed ignition temperatures $\vartheta_z = 500$ and 200° C the data of table 6.

---

[1]For propane, λ was linearly interpolated between 0.013 at 0° C and 0.080 at 500° C. The first figure was interpolated from the series CH_4, C_2H_6, i-C_5H_{12} with $\lambda = 0.026 \rightarrow 0.0155 \rightarrow 0.0105$ (Chem. Ing. I, 1, 1933, p. 323) and is in agreement with the Landolt-Börnstein data. The value 0.080 at 500° C was estimated from the kinetic gas formula $\lambda = \frac{1}{3} c^* l^* \rho c_1$, ($c^*$, mean molecular velocity, l^*, mean free wave length, c_1, effective specific heat (cf. reference 8, vol III, 2, 1925, p. 92) on the assumption that at transition from 0° C to 500° C the expression $\frac{1}{3} c^* l^* \rho$ is doubled (exactly as for oxygen, where the effective specific heat c_1 remains practically constant) and that c_1 is tripled.

[2]For oxygen, λ at 500° C is not known, for nitrogen, it is 0.040. The oxygen values are a little higher on the whole; so the value 0.044 ± 0.006 is probably correct.

TABLE 6

ϑ_z °C	δ_v cm	$\left(\frac{\partial \vartheta}{\partial x}\right)_z$ grad cm^{-1}	$\bar{U}$ mol fuel/cm^3 sec	δ_R cm
500	$(3.5\pm0.6)\times10^{-3}$	$(5.0\pm1.3)\times10^{5}$	$\frac{1}{f}\times(0.40\pm0.10)$	$f\times(5.0\pm1.5)\times10^{-3}$
200	$(3.3\pm0.3)\times10^{-3}$	$(2.6\pm0.3)\times10^{5}$	$\frac{1}{f}\times(0.18\pm0.02)$	$f\times(10.9\pm1.3)\times10^{-3}$

The cited limits of error correspond to the uncertainty of the employed $\bar{c}_p$, λ and λ_z values.

An objection may be raised against the thus computed values: for for it is questionable whether these $\bar{c}_p$ and λ values, obtained experimentally on slow processes, are still applicable to the speedier processes in the flame. On the one hand, the preheating takes place within about $\frac{3\times10^{-3}}{300} = 10^{-5}$ sec, whereby a single molecule receives only about 10^5 impulses. On the other hand, it is a known fact that a molecule, in order to change its vibrational quanta to translation energy must receive from 10^4 to 10^5 impulses, and that this figure is never less except in special cases; and that is, when at the impulse, so to say, the complex of a chemical compound able to exist is preparatorily formed (reference 10). It is therefore entirely conceivable that smaller $\bar{c}_p$ and λ values with only partial or not at all excited vibrational heats are valid for the flames. The latter case can be quantitatively computed, when it is remembered that, by kinetic gas theory, molal heat $\underline{C}_p$ and thermal conductivity λ are represented in the following manner: for complete adjustment of the vibrational quanta:

$$\underline{C}_p = \underline{C}_t + \underline{C}_r + \underline{C}_s + \underline{R} \tag{16}$$

$$\lambda = k\underline{C}_1 = k\left[2.5\,\underline{C}_t + \underline{C}_r + \underline{C}_s\right] \tag{17}$$

for unadjusted vibrational quanta:

$$\underline{C}_p' = \underline{C}_t + \underline{C}_r + \underline{R} \tag{18}$$

$$\lambda' = kC_1 = k\left[2.5\,C_t + C_r\right] \tag{19}$$

where K is a constant solely dependent on the mean molecular speed c^*, the free path length l^*, and the density ρ(reference 8), and R is the gas constant $\underline{C}_t$ the translational portion, $\underline{C}_r$ the rotational portion and $\underline{C}_s$ the vibrational portion of the molal heat. Quantity $\underline{C}_1$

identifies the effective molal heat to be inserted in the kinetic gas term for thermal conductivity according to Chapman and Enskog. Therefore, in general:

$$\underline{C}_1 - \underline{C}_p = \underline{C}'_1 - \underline{C}'_p = 1.5\,\underline{C}_t - \underline{R} = 2.5 \text{ cal/mol grad} \tag{20}$$

The numerical values obtained by this method are reproduced in table 7; the values for the gas mixtures were computed additively from the values of the individual components by the mixing rule.

TABLE 7

C	Propane				Oxygen				Mixture: 15 percent propane 85 percent oxygen			
	$\underline{C}_p$	$\underline{C}'_p$	$\underline{C}_1$	$\underline{C}'_1$	$\underline{C}_p$	$\underline{C}'_p$	$\underline{C}_1$	$\underline{C}'_1$	$\underline{C}_p$	$\underline{C}'_p$	$\underline{C}_1$	$\underline{C}'_1$
100	16.4	8.0	18.9	10.5	7.15	7.0	9.65	9.5	8.54	7.15	11.04	9.65
200	22.0	8.0	24.5	10.5	7.38	7.0	9.88	9.5	9.57	7.15	12.07	9.65
250	24.8	8 0	27.3	10.5	7.5	7.0	10.0	9.5	10.1	7.15	12.59	9.65
500	35.0	8.0	37.5	10.5	8.0	7.0	10.5	9.5	12.1	7.15	14.55	9.65

Noting that according to equations (19) and (14)

$$\delta_v \sim \frac{\lambda}{\bar{c}_p} \sim \frac{\underline{C}_1}{\underline{C}_p} \tag{21}$$

and

$$\delta_R \sim \frac{\lambda_z}{\bar{c}_p} \sim \frac{\underline{C}_{1z}}{\underline{C}_p} \tag{22}$$

and identifying the quantities computed with the unadjusted vibration quanta by a dash as before gives for the calculated mixture values of table 7

$$\text{for } \vartheta_z = 500^\circ \text{ C: } \frac{\delta'_v}{\delta_v} = \frac{C'_{250}}{C_{p250}} \frac{C_{p250}}{C_{1250}} = 1.08 \tag{23}$$

and

$$\frac{\delta'_R}{\delta_R} = \frac{C'_{1500}}{C_{p250}} \frac{C_{p250}}{C_{1500}} = 0.94 \tag{24}$$

$$\text{at } \vartheta_z = 200^\circ \text{ C: } \frac{\delta'_v}{\delta_v} = \frac{C'_{1100}}{C'_{p100}} \frac{C_{p100}}{C_{1100}} = 1.04 \tag{25}$$

and

$$\frac{\delta_R'}{\delta_R} = \frac{c_{l200}'}{c_{p100}'} \frac{c_{p100}}{c_{l200}} = .96 \qquad (26)$$

Thus the calculated thicknesses of the preparatory and the reaction zone vary very little, if in place of the complete vibration adjustment only a limited one or none at all is assumed.

For δ_R, of course, yet another possibility is involved, namely, that in equation (14) the vibrational heat is completely adjusted for c_p but not for λ_z. For according to the physical derivation of equation (14) from equations (7) and (13), c_p refers to the whole preparatory zone, and the gas particles remain longer in it than in the immediate vicinity of the place of ignition where λ_z is to be formed. For the reaction zone thicknesses δ_R'' computed with this somewhat extreme assumption the result is

at $\vartheta_z = 500^\circ$ C: $$\frac{\delta_R''}{\delta_R} = \frac{c_{l500}'}{c_{p250}} \frac{c_{p250}}{c_{l500}} = 0.66 \qquad (27)$$

at

$$\vartheta_z = 200^\circ \text{ C}: \quad \frac{\delta_R''}{\delta_R} = \frac{c_{l200}'}{c_{p100}} \frac{c_{p100}}{c_{l200}} = 0.80 \qquad (28)$$

In this instance the δ_R'' would therefore be smaller than the previously calculated δ_R, but by no means greater.

These considerations show that the zones of preparation and reaction defined by equations (10) and (14) are still comparatively accurately computable, although the data for the specific heats and thermal conductivities are not too accurately known, and although it is not even decided whether the degrees of freedom of vibration of the molecules during the brief intervals in the flame front are excited completely, little, or not at all.

A somewhat closer observation is necessary for the rate of chemical reaction U on the one hand, and the thicknesses δ_R and $\delta_v+\delta_R$ on the other. The rate of chemical reaction

$$\bar{U} \approx 0.2 \text{ mol cm}^{-3} \text{ sec}^{-1}$$

is quite high; because, when it is remembered that in the reaction zone on an average, fuel of the order of magnitude of 2×10^{-6} molecules per cubic centimeter is present (at start $n_{ba} = 6.7\times10^{-6}$ mol/cm^3)

a mean combustion period of $\frac{2 \times 10^{-6}}{0.2} = 10^{-5}$ sec is obtained.

This period is extremely short compared with the reaction periods for which investigation methods worked out so far, exist. For, in kinetic reaction studies by the static method (closed off reaction vessel in which the progress of the reaction is followed by observation of the pressure variation or some other physical property) time intervals down to only about 1 second can be followed up; by the conventional flow method it succeeds only to about 10^{-2} or 10^{-3} second; insofar as reasonably defined pressure and temperature conditions in the reaction zone are demanded. Nevertheless, a reaction period of 10^{-5} second is still not the shortest one conceivable for a combustion process, because a fuel particle still receives about 10^5 impulses during this period. Hence, if 10^2 impulses on a fuel particle were sufficient for its complete decomposition, which is entirely conceivable with correspondingly energy-rich and adequate impulse partners, the rate of combustion would have to be 10^3 times higher. Such enormously fast combustion processes have, in fact, been actually observed, namely, at detonations, where the speed of travel of the flame front is counted by kilometers per second; while at the normal speeds of ignition in the Bunsen flame a few millimeters per second are sufficient.

Hydrodynamically a comparison of the thickness of the preparatory zone δ_V and the reaction zone δ_R with the size of the turbulence bodies occurring in the turbulent flow (gas bodies with occasionally uniform velocity vector) is interesting.

Interesting from the point of view of chemical reaction is the comparison of the theoretical guantities δ_V and δ_R with the experimentally directly observed thickness of the luminous zone δ_L. It was established at $(10 \pm 2) \times 10^{-3}$ centimeter in the previously reported tests, which is, within the limits of error, independent of the propane concentration. Nor was there any indication that these luminous zones were artificially enlarged for the eye or the photographic plate by any flickering motion of the flame. In consequence the following possibilities exist according to table 6:

$\left.\begin{array}{l} \delta_L \approx d_V + \delta_R \text{ if } \vartheta_Z = 500^\circ \text{ C} \\ \qquad \text{and } f = 1 \text{ case I} \end{array}\right\}$ assumption A

$\left.\begin{array}{l} \delta_L \approx \delta_R \text{ in case that } \vartheta_Z = 500^\circ \text{ C} \\ \qquad \text{and } f = 2 \text{ case II} \\ \delta_L \approx \delta_R \text{ in case } \vartheta_Z = 200^\circ \text{ C} \\ \qquad \text{and } f = 1 \text{ case III} \end{array}\right\}$ assumption B

Which one of these three cases actually obtains has not been definitely decided as yet, especially as it is not known in what manner the emitted spectra are distributed over the individual sections of the luminous zone.[1] But tentatively two assumptions A and B may be made:

A. Luminosity extends over preparation and reaction zone; in which case 500° C should be assumed as ignition temperature, according to table 6, that is, a value which, in contrast to previous arguments, approximately corresponds to the ignition temperatures obtained by Nernst's method for adiabatic compression or with the Dixon burner. But it would be difficult to explain why the luminosity in the preparatory zone, where there is practically no chemical conversion, should appear with about the same intensity as in the reaction zone.

B. Luminosity occurs only in the reaction zone: in case II with $f = 2$, $\vartheta_Z \approx 500°$ C would then have to be assumed as ignition temperature (cf. table 6), that is, the same high ignition temperature as with assumption A, or else $\vartheta_Z \approx 200°$ C in case III with $f = 1$, that is, a substantially lower ignition temperature. Case II is, however, less probable. While it would yield a reaction thickness δ_R which agrees with the thickness of the experimental luminous zone δ_L (table 6), this thickness δ_R would not be uniformly luminous, but practically only on the first half. For, when it is assumed that luminosity occurs only in the reaction zone, its intensity is presumably parallel with the chemical conversion and hence with the momentary temperature gradient $\frac{\partial \vartheta}{\partial x}$ in the reaction zone δ_R[2]. But its course differs considerably in both cases II and III; that is, in case II the high values of the temperature gradient occur only on the first half of the reaction zone, while in case III the temperature gradient is approximately constant over the thickness δ_R. This is readily apparent when the temperature curve for both cases is plotted (figs. 7(a) and 7(b))since absolute value and temperature gradient for starting point and end point of δ_R are known. (See table 6. Note that $\frac{\partial \vartheta}{\partial x}$ must equal 0 for $x = \delta_R$[2].)

---

[1] If, for instance, at the beginning of the luminous zone spectra other than those of OH, CH, and C_2 were found in appreciable quantities, an encroachment of the luminous zone upon the preparation zone would be quite probable.

[2] Of course, it could be assumed for the present that a particle is luminous at a later place than where it is energetically excited, and that through it the luminous zone would be wider than the area of the maximum temperature gradient. But this type of enlargement is surely entirely negligible; because the excited particle has but a lifetime of about 10^{-8} second, after which it radiates its energy, and in this interval it would have traversed exactly 1/1000 of the total reaction zone thickness δ_R.

Comparison of the experimental δ_L with the theoretical δ_v and δ_R values leads to the very probable final result:

The experimentally defined luminous zone δ_L either extends to the preparatory zone δ_v and to the reaction zone δ_R. In this case the ignition temperature ϑ_z in the flame is almost exactly as high as by Nernst's method of adiabatic compression or with the Dixon burner. Or the luminous zone δ_L covers only the reaction zone δ_R, in which instance the ignition temperature ϑ_z in the flame is lower than for adiabatic compression or with the Dixon burner

Of these two cases the latter is, for the time being, held to be more likely. Further elucidation is, first of all, to be expected from the spectroscopic side, where type and intensity distribution of the spectra in the luminous zone would have to be explored.

3. Enlargement of a Laminar Free Jet and Form of Bunsen Cone Possible in It

In order to obtain the form of the flame surface of a Bunsen flame quantitatively, for laminar flow, the simple free jet without combustion is considered and it is proved that, under the previously employed experimental conditions (Re > 600), its enlargement at a distance of several tube diameters, corresponding to the height of the measured flame cone is very insignificant.

According to an article on laminar jet expansion by H. Schlichting (reference 11) the half-value width $2b$[1] of the velocity profile (cf. fig. 8, which was taken from that report) depends only on the kinematic total momentum K, on the kinematic viscosity ν, and on the distance x conformably to the equation

$$\frac{2b}{x} = 2.57 \sqrt{\frac{16\pi}{3K}}\ \nu \tag{29}$$

with

$$K = \int_0^\infty 2\pi\, u^2 r\, dr \tag{30}$$

[1]In the radial distance b the velocity is occasionally half as great as on the jet axis, equal flow cross section being assumed.

Of course, equation (29) applies, for the first, only to a jet that issues from an infinitely small orifice, but even so it can be applied to the case of a jet from a finite pipe cross section, when the left-hand side of equation (29) is regarded as a measure for the jet expansion. The kinematic momentum which must be the same on all subsequent jet cross sections according to equation (30) can then be summarily calculated for the stationary pipe flow with parabolic velocity profile:

$$K = \int_0^{\infty} 2\pi\,(2\bar{u})^2\left[1 - \left(\frac{r}{R}\right)^2\right]^2 r\,dr \qquad (31)$$

$$= \frac{4\pi\,\bar{u}^2 R^2}{3} = \frac{\pi}{3}\,\bar{u}^2\,d^2$$

By insertion in equation (29):

$$\frac{2b}{x} = 2.57\sqrt{\frac{16\pi}{3}\,\frac{3}{\pi\bar{u}^2 d^2}}\;\nu = \frac{10.28}{Re} \qquad (32)$$

The relative expansion of the laminar free jet issuing at the Reynolds number Re from a tube is therefore inversely proportional to it, and at the lowest value Re = 612 of the present tests becomes

$$\frac{2b}{x} \leq \frac{10.28}{612} \approx \frac{1}{60} \qquad (33)$$

This is very little, so that there can be no perceptible variation of the velocity profile at a distance of a few tube diameters from the orifice. The combustion zone will, of course, modify the flow conditions in the hot part beyond the cone of the flame very substantially. But on its inside, that is, between this and the pipe orifice, the original velocity profile is scarcely altered; for this would involve the variation of a flow pattern before a center of disturbance (that is, the surface of the flame), and such changes are usually small, unless the center of disturbance necessitates a complete deflection of the flow, which, however, is not the case here.

Thus the assumption that all gas particles enter the surface of the flame at the same rate of flow at which they have left the orifice of the burner tube appears to be justified.

Now the shape of the flame surface can be calculated when it is assumed that the flame speed w_{fl} is the same at all points and first

becomes abruptly zero at the base. (See reference 4, p. 46; also reference 12.)

For every single surface element of the flame cone with the horizontal and vertical coordinates r and h there results in analogy to equation (1):

$$w_{fl}\, 2\pi\, r \sqrt{1 + \left(\frac{dh}{dr}\right)^2}\, dr = u\, 2\pi\, r\, dr \qquad (34)$$

or, considering the parabolical velocity profile in laminar flow (with average flow velocity $\bar{\bar{u}}$)

$$u = 2\bar{\bar{u}}\left[1 - \left(\frac{r}{R}\right)^2\right] \qquad (35)^1$$

$$\frac{d(h/R)}{d(r/R)} = -\sqrt{\left(\frac{2\bar{\bar{u}}}{w_{fl}}\right)^2 \left[1 - \left(\frac{r}{R}\right)^2\right]^2 - 1} \qquad (36)$$

The last relation was graphically integrated for various assumed values of $\frac{\bar{\bar{u}}}{w_{fl}}$ and the cone forms illustrated in figure 9 ascertained. They are not in complete agreement with the experimental flame cones, as is especially noticeable from figure 10, where experiment no. 47 – for which

$$\frac{\bar{\bar{u}}}{w_{fl}} = \frac{638}{128} = 4.98 \text{ and } \frac{638}{100.8} = 6.33$$

is exactly valid (cf. table 3) is compared with the theoretical curve for $\frac{\bar{\bar{u}}}{w_{fl}} = 6$. Two substantial differences were noted:

(a) The base of the experimental flame cone not only covers, as in the theoretical case, the internal burner tube cross section, but reaches beyond it.

(b) The upper end of the experimental flame cone is, in contrast to the theoretical, rounded off and lies considerably lower.

---

[1]The gas is assumed to be at rest at the pipe wall; whereas Michelson, who made the first calculations of this kind, erroneously took the possibility of a perceptible sliding into consideration.

Finding (a) is probably explainable as follows: immediately above the rim of the burner orifice where the gas, owing to adequate heat removal by the burner tube, cannot ignite, a considerable radial and outwardly directed flow must exist, since there is always a higher pressure p_a inside of the flame cone than outside (p_e). This radially discharging gas cannot ignite until it is a certain distance away from the burner tube, and thus the base of the flame cone is drawn out over the burner orifice. The pressure difference is, according to the momentum theorem (reference 4, p. 44):

$$p_a - p_e = \rho_a w_f^2 \left(\frac{\rho_a}{\rho_e} - 1\right) \tag{37}$$

hence for experiment 47, illustrated in figure 10, with

$$\rho_a = 1.50\times10^{-3}\ \text{gram centimeter}^{-3},\quad w_f = 114.4\ \text{centimeter sec}^{-1}$$

and

$$\frac{\rho_a}{\rho_e} = \frac{\vartheta_e + 273}{\vartheta_e + 273} = \frac{3273}{273} = 12:$$

$$p_a - p_e \approx 1.50\times10^{-3}\times1.31\times10^{4}\times11\ \frac{\text{dyn}}{\text{square centimeters}}$$

$$= 216\ \frac{\text{dyn}}{\text{square centimeters}} = 0.22\ \text{centimeter } H_2O \tag{38}[1]$$

This pressure difference is quite considerable. If it is regarded as dynamic pressure at density ρ_a, a velocity w can be correlated, which should represent an approximate measure for the radial, outwardly directed velocity immediately above the burner tube rim. Hence from equation (37)

---

[1]For a stoichiometric mixture of 16.7 percent propane, the rest oxygen, it would give

$$\rho_a = 1.44\times10^{-3}\ \text{g cm}^{-3};\ w_f = 300\ \text{cm s}^{-1};\ \frac{\rho_a}{\rho_e} \approx 12,\ \text{and hence}$$

$$p_a - p_e = 1425\ \frac{\text{dyn}}{\text{cm}^2} = 1.45\ \text{cm } H_2O!$$

$$\left.\begin{aligned} \frac{\rho_a \underline{w}^2}{2} &= \rho_a w_f^2 \left(\frac{\rho_a}{\rho_e} - 1\right) \\ \text{or} \qquad \underline{w} &= w_f \sqrt{2\left(\frac{\rho_a}{\rho_e} - 1\right)} \approx 4.7\, w_f \end{aligned}\right\} \quad (39)$$

The last relation is as yet not to be found in the literature. Still, it is important, because it makes it possible to decide forthwith whether or not air from the outside can diffuse in the inside of the cone through the free slit between burner tube rim and flame cone base. In general, the negative seems to be the case. For on assuming even the very small value $x = 0.01$ centimeter for the radial thickness of the diffusion layer and $D = 0.2$ square centimeter per second for the diffusion coefficient of air, the inward rate of diffusion of the air particles would be

$$\frac{D}{x} = \frac{0.2}{0.01} = 20 \text{ centimeters per second} \quad (40)$$

against the radially outward flow velocity of $\underline{w} = 4.7 \times 114 = 536$ centimeters per second.

Naturally, it is also conceivable that the gas portions flowing radially outward above the burner tube rim reach combustion only after appreciable mixing with the surrounding air. They would burn slower or faster (slower for initially poor mixtures, faster for initially rich mixtures). The recorded flame velocities could be so much more faulty as the gas portion, converted in the lowest border zone of the experimentally surveyed flame cone, is greater. This effect should be watched particularly on small burner tube diameters, although it did not seem to have any part in the previously reported measurements. The laminar flame speeds obtained with burner tubes I($d = 0.1385$ centimeter) and II ($d = 0.218$ centimeter) are satisfactorily grouped within the limit of error of about ±10 percent about the dashed curve of figure 5.

Finding (b), the rounded off and lower position of the upper end of the experimental flame cone (cf. fig. 10) is perhaps due to the fact that the flame speed w_f at the cone tip is higher than on the rest of the surface elements of the cone envelope. The gas particles which reach combustion in the cone tip receive heat and active chain carriers not only from this tip itself but also from the immediately adjacent parts of the enveloping surface, so that ignition and hence combustion itself are facilitated. This interpretation is particularly supported by the fact that the curvature radii at the upper end of the measured flame cones are of the same order of magnitude as the thicknesses of the luminous zones, namely, 0.01 centimeter.

4. Prandtl's Exchange Quantity and Mixing Length in the Turbulent Free Jet (Nuclear and Marginal Turbulence)

α. General considerations.– According to Prandtl the developed turbulence of a stationary flow can be identified in every point of the field of flow by two locally dependent quantities, that is, the mixing length l and the turbulent exchange quantity . The former is defined as length and represents the approximate mean diameter of the turbulence bodies (that is, areas of closely spaced particles, which occasionally manifest a uniform vector of the flow velocity); the latter is an effective diffusion coefficient of the dimension square centimeters per second (reference 13). The introduction of these two quantities is based upon the analogy of all transport processes in a gas at rest and in a turbulently flowing medium, so far as they are superposed at least in the latter case, on the principal flow. These transport processes (that is, diffusion = transport of a certain type of particle, viscosity = transport of momentum, thermal conduction = transport of energy) are reduced in both cases to irregular motions, in the case of still gas to the gas molecule, in the case of turbulent medium to that of the turbulence body. In still gas the individual gas molecules move irregularly at a mean velocity c^* and traverse the mean free path length l^* between two collisions. In turbulent flow the individual turbulence bodies possess, aside from the stationary mean flow velocity $\bar{w}$, an irregular, rapidly changing additional velocity $\bar{w}'$, and they maintain these speeds on the average occasionally over a path length l, the mixing length.

Just as the diffusion coefficient in the kinetic gas theory, is defined as

$$D = \frac{1}{3} \, l^* \, c^* \tag{41}$$

so Prandtl defines his exchange quantity at

$$\epsilon = l \, \bar{w}' \tag{42}$$

$|\bar{w}'|$ is the time average value (denoted by upper dash) of the absolute amount of w'[1]. The kinetic gas factor 1/3 in equation (41) is included

---

[1]Averaging over $|w'|$ is necessary, because the time average value of w' disappears by definition.

in equation (42) in the quantities l and $|\overline{w'}|$, which is physically correct, since, the mixing length l in the turbulent flow must, for reasons of continuity, be of the same order of magnitude as the diameter of the turbulence bodies, and this diameter cannot be arbitrarily defined, because every one of these gas bodies is enveloped by a more or less thick marginal zone in which the different flow altitudes of the adjacent bodies are continuously adopted.

Numerical values for the exchange quantity ϵ can be secured in several ways. For very rough estimates it is sufficient, for instance, to determine quantity l and $|\overline{w'}|$ separately in equation (42) (for instance, by hot-wire measurements and determination of the correlation coefficient for the concurrent velocity fluctuations at two adjacent points)[1] and then simply multiply these values with each other. But this affords only the order of magnitude of ϵ, since the turbulence body diameters l must be indicated with wider margin. Exact values for ϵ are obtainable by surveying a specific transport process in the turbulent flow. Only such ϵ values as those obtained by the latter method are used in the following study.

Consider the specific case of a one-dimensional principal flow ($\overline{w} = u\underline{i} + v\underline{j} + w\underline{k}$ with $v = w = 0$), superposed by the turbulent velocity fluctuations $\underline{w}' = u'\underline{i} + v'\underline{j} + w'\underline{k}$, and assume that the unit mass of the flowing medium at any one point has the additive property s — expressible by a digit — of varying from place to place. Then, if $\frac{\partial s}{\partial y} \neq 0$ conformably to figure 11, a "property flow $\underline{s}_y$" transverse to the principal flow direction $\underline{i}$ can be computed, that is, the amount of property s which is transported in unit time per unit surface in the j-direction

$$\underline{s}_y = |\overline{v'}| \left[\rho s \frac{l}{2} \frac{\partial(\rho s)}{\partial y} \right] - |\overline{v'}| \left[\rho s + \frac{l}{2} \frac{(\rho s)}{\partial y} \right] \qquad (43)$$

$$= - l \, |\overline{v'}| \, \frac{\partial(\rho s)}{\partial y}$$

or, with equation (42) taken into consideration:

---

[1]On a wheat field waving in the wind the turbulence bodies of the air current are directly delineated, so that for this case the magnitude of the bodies and — by allowance for the mean wind velocity — the mean velocity fluctuation $|\overline{w'}|$ can be given.

$$\underline{s}_y = \epsilon \frac{\partial(\rho s)}{\partial y} \tag{44}$$

If, for instance, s signifies the mean momentum per unit mass in principal flow direction (hence $s = \overline{u}$), then $\underline{s}_y$ becomes the shearing stress τ transmitted transverse to the principal flow direction, and with it for incompressible fluid

$$\tau = \rho\epsilon \frac{\partial \overline{u}}{\partial y} \tag{45}$$

which means, however, that the exchange quantity ϵ can be immediately specified, when the local shearing stress distribution for the particular flow and the velocity distribution $\overline{u}$ have been measured. If s in in equation (44) indicates the enthalpy $s = c_p \vartheta$ of a practically incompressible fluid referred to any one zero point,

$$\underline{s}_y = -c_p \rho \epsilon \frac{\partial \vartheta}{\partial y} \tag{46}$$

represents a heat flow, and hence yields an effective thermal conductivity coefficient in the turbulent flow:

$$\lambda_{turb} = c_p \rho \epsilon \tag{47}$$

Lastly, if the number $\overrightarrow{N_k}$ of particles of type k, which alone is transported by turbulent mixing motion in a concentration vessel $-\frac{\partial n_k}{\partial y}$ in y-direction per unit time and surface is of interest, then

$\underline{s}_y = \overrightarrow{N_k}$ and $\rho s = n_k$ are written in equation (44), so that

$$\overrightarrow{N_k} = -\epsilon \frac{\partial n_k}{\partial y} \tag{48}$$

This equation makes it particularly plain that ϵ is a quantity of the type of a diffusion coefficient.

But in the following not only the exchange quantity ϵ, but also the mixing length l is of interest, although it gives the turbulence body diameter only in order of magnitude; for l undoubtedly represents a characteristic length for the turbulent flow, just as the preparatory zone thickness δ_V and the reaction zone thickness δ_R constituted characteristic lengths of the stationary flame front in laminar flow. Quantity l can be determined from the correlation of the velocity

fluctuations on two adjacent points, as previously stressed. However, Prandtl and his school used in part a different method. Prandtl had found from continuity considerations that in the one-dimensional principal flow

$$\overline{v'} = l\left|\frac{\partial \bar{u}}{\partial y}\right| \tag{49}$$

must approximately apply; whence for the exchange quantity

$$\epsilon = l^2 \left|\frac{\partial \bar{u}}{\partial y}\right| \tag{50}$$

or by insertion in equation (45):

$$\tau = \rho l^2 \left|\frac{\partial \bar{u}}{\partial y}\right| \frac{\partial \bar{u}}{\partial y} \tag{51}$$

In the last equation, τ, ρ and $\frac{\partial \bar{u}}{\partial y}$ are experimentally accessible, so that l can be computed immediately.

Equations (45) and (51) formed the initial equations by which the quantities ϵ and l, in the subsequently discussed reports, were determined.

β. Nuclear and marginal turbulence in a free jet.- The interpretation of the flame phenomena observed in turbulent flow stipulates ϵ and l as functions of the location for the turbulent free jet issuing stationarily from a tube. Although this case has up to now not been explored experimentally in its entirety, two other cases are known:

a. The turbulence in a circular pipe in stationary flow was experimentally investigated by J. Nikuradse and the ϵ and l values determined (reference 14).

b. The turbulence in the mixing zone between a turbulent free jet and the bordering still air was theoretically explored by Tollmien (reference 2); he found the sole constant still undetermined in the theory by comparison with Gottingen wind-tunnel measurements (reference 15), so that here also, the two factors l and ϵ, are known. Thus the turbulence conditions in the free jet can be immediately surveyed when assuming that the jet can be decomposed in a nuclear and a marginal flow, and that in the former the unchanged turbulence condition of the simple pipe flow is still maintained (according to a). This decomposition cannot, of course, apply to any desired great distance x from the tube orifice, because the marginal zone expands continuously, while

the nuclear flow shrinks conically. But it will be seen that an essential part of the turbulent combustion phenomena (and this is precisely the most interesting part) still falls in the zone of the nuclear flow.

Figures 12 and 13 show the nuclear turbulence in a free jet in diagrammatic representation. In figure 12 the dimensionless exchange quantity $\frac{\epsilon}{\bar{\bar{u}}R}$ ($\bar{\bar{u}}$ is flow velocity averaged over the tube cross section and with respect to time; R, tube radius) is plotted against the relative distance from the tube axis $\frac{r}{R}$;[1] in figure 13 the mixing length $\frac{l}{R}$ made nondimensional with the tube radius is also plotted against $\frac{r}{R}$. It is seen from figure 12 that ϵ is not maximum at the tube center line but approximately at distance $r = \frac{1}{2}R$. This fact can be regarded as an experimental confirmation of the approximate formula (49); for the closer the approach to the tube axis, proceeding from the wall, the greater the reduction in $\left|\frac{\partial \bar{u}}{\partial y}\right|$, and since l cannot grow indefinitely, ϵ must again decrease.

According to figure 13 the mixing length is less than 8 percent of the tube diameter, hence less than 0.16 millimeter for a 2-millimeter burner tube. Accordingly the turbulence bodies would, in consideration of the nonarbitrary definition of their diameters, definitely come within the order of magnitude which had been found for the thickness of the laminar flame zones.

The nondimensional quantities $\frac{\epsilon}{\nu}$ and $\sqrt{\frac{\epsilon}{\nu}}$ employed later,[2] are reproduced in table 8 for nuclear flow at different Reynolds numbers and different $\frac{r}{R}$.

---

[1]Nikuradse's graphical representation could not be used direct, because he used the so-called "shearing stress velocity v*" to make ϵ dimensionless, which, however, is not so suitable for the present purpose as the mean flow velocity $\bar{\bar{u}}$.

[2]According to the kinetic gas theory the kinematic viscosity ν is approximately equal to the diffusion coefficient D; for a pure gas the agreement is complete.

The marginal turbulence at the boundary of a free jet was explored by Tollmien on the streamline pattern illustrated in figure 14. This does not completely correspond to the boundary conditions of the present tests, which involved the exit of a free jet from a tube of finite wall thickness and tapered at the orifice, rather than the discharge of a free jet from a straight wall (visualized as being placed perpendicular to the plane of drawing through the y-axis) as in figure 14. Nevertheless, an analysis of Tollmien's case is interesting. The two-dimensional plane problem which Tollmien first investigated and which presents the greatest interest, involved the solution of the differential equations

$$\frac{\partial u}{\partial x} + \frac{\partial v}{\partial y} = 0 \tag{52}$$

and

$$u \frac{\partial u}{\partial x} + v \frac{\partial u}{\partial y} = \frac{1}{\rho} \frac{\partial \tau_{xy}}{\partial y} \tag{53}$$

with the shearing stress

$$\tau_{xy} = \rho k^2 x^2 \frac{\partial u}{\partial y} \frac{\partial u}{\partial y} \tag{54}$$

Herein k is a temporarily unknown constant in the formula for the mixing length

$$l = k\,x \tag{55}$$

The differential equations were solved by means of a stream function for the velocities u and v, without going into any further details. Only the most important result is repeated here: namely, the entire marginal zone lies in a sector, the tip of which is located at the tube end (inside wall of tube) and this is bounded by the two straight lines

$$y_1 = 0.981 \sqrt[3]{2k^2x} = b_i \tag{56}$$

$$y_2 = -2.04 \sqrt[3]{2k^2x} = -b_a \tag{57}$$

For $y > y_1$ the flow velocity is $u = \bar{u}$, for $y < y_2$, $u = 0$. Hence for the total width of the mixing zone distant x from the mouth of the tube

$$b = b_1 + b_a = 3.02 \sqrt[3]{2k^2x} \tag{58}$$

The best agreement with the experiments of the Göttingen wind-tunnel measurements was obtained with

$$\sqrt[3]{2k^2} = 0.845 \text{ and } k = 0.0174 \tag{59}$$

which gives a mixing length

$$l = 0.0174\, x = 0.0682\, b \tag{60}$$

The mixing length in the marginal zone therefore amounts to about 7 percent of its momentary thickness, while l in the nuclear zone of the free jet was established at less than 8 percent of the tube diameter. In addition

$$b_i = 0.83x; \quad b_a = 0.172x; \quad b = 0.255x \tag{61}$$

From the first equation (61) it follows that for $x = 12$ R = 6 d the inner part b_i of the marginal zone is equal to R, that is, the marginal zone here reaches the original tube axis, so that the area of the nuclear flow with the original turbulence conditions in the tube disappears.

Inside of the mixing zone b the flow velocity u drops in first approximation from its original value $\bar{\bar{u}}$ in nuclear flow to the value 0 in still air, thus realizing the trapezoidal velocity profiles for the free jet, as experimentally observed. With this the turbulent exchange quantity is

$$\epsilon = l^2 \frac{\partial u}{\partial y} \sim \frac{l^2 \bar{\bar{u}}}{b} = \frac{0.0174^2 \bar{\bar{u}} x}{0.255} = 1.188 \times 10^{-3}\, \bar{\bar{u}}\, x \tag{62}$$

or nondimensionally expressed, when the Reynolds number of the tube flow $R = \frac{\bar{\bar{u}} d}{\nu}$ is introduced:

$$\frac{\epsilon}{\nu} = 1.188 \times 10^{-3} \times \mathrm{Re}\, \frac{x}{d} \tag{63}$$

This treatment of the free-jet marginal zone is, of course, not completely exact, inasmuch as the calculation was based upon the plane case in contrast to the really interesting marginal zone which is curved at right angles to the x, y-plane of figure 14. Hence, the closer the inner part b_i of the marginal zone approaches the radius of the tube, the greater the discrepancies between the computed ϵ and l values that must be expected. Owing to this very uncertainty the exact $\left|\frac{\partial u}{\partial y}\right|$ values were not written in equation (62), although it would have been entirely possible on the basis of Tollmien's results, but the average value $\left|\frac{\partial u}{\partial y}\right| \approx \frac{\bar{\bar{u}}}{b}$. This also meant a great saving in paper work. On the

other hand, the exchange quantities and mixing lengths calculated by equations (62) and (60) cannot be too far wrong, for in the report cited Tollmien also treated the case of the rotationally symmetrical free jet that emerges from an infinitely small orifice. The mixing zone then assumes the shape of a cone with straight enveloping surface. The mixing length at distance x from the point of discharge is

$$l' = 0.0158\ x \tag{64}$$

and the momentary cone radius

$$r' = 0.214\ x \tag{65}$$

This mixing length differs from that used above ($l = 0.0174\ x$) by only 9 percent, while the cone radius r' differs by a mere 16 percent from the previous width of marginal zone $b = 0.255\ x$.[1] And the exchange quantities computed with the values (64) and (65) differ even less from the others, that is, only 2 percent: for the insertion in equation (62) gives

$$\epsilon \approx \frac{l'^2 \bar{u}}{r'} = \frac{0.0158^2 u x}{0.214} = 1.168 \times 10^{-3} \bar{u}\ x \tag{66}$$

The values of $\frac{l}{R}$ and $\frac{\epsilon}{\nu}$ computed by equations (60) and (63) are given in table 8 for different Reynolds numbers of tube flow and for different relative distances $\frac{x}{R}$ from the mouth of the tube. Column 2, containing $\frac{b_i}{R}$, shows immediately the extent to which the marginal zone has penetrated into the area of the original nuclear flow. With the data of the nuclear zone on top, and the data on the marginal zone below, the turbulence properties in the two-flow regions can be directly compared. An even better insight is afforded from figure 15, where the nondimensional exchange quantity $\frac{\epsilon}{\nu}$ (solid curve) and the nondimensional mixing length $\frac{l}{R}$ (dashed curve) for nuclear and marginal flow are shown plotted against different $\frac{x}{R}$.[2] It is interesting to note that in the vicinity of the tube orifice (for $\frac{x}{R} < 4$) the turbulence in the nuclear

---

[1]The cone radius r' must be compared with the thickness b for the reason that at the place where the region of the nuclear flow is absorbed by that of the marginal flow, the total width of the free jet is exactly $2r'$ and $2b$, respectively.

[2]The discontinuous transitions between marginal and nuclear zone and between marginal zone and the outer quiescent medium manifested by the ϵ and l curves in figure 15 are attributable to the simplifying assumptions in the present estimation, which naturally describes the true conditions only in first approximation.

zone is greater than in the marginal zone, both as regards exchange quantity ϵ and mixing length l. But as the distance from the tube orifice increases, the ϵ values of the marginal zone very quickly overtake those of the nuclear zone, that is, the more the latter is absorbed by the first, the closer its mixing lengths approach. At the point where the nuclear zone disappears the mixing lengths in the nuclear and marginal zone are practically alike. This fact is noteworthy, for it means that the numerical values derived from two entirely independent reports by Tollmien and Nikuradse are not merely compatible but even supplement each other. This is a necessary condition if the turbulence estimate which is based on the estimates in two partial zones is to represent the actual conditions to some extent.

5. The Several Theoretically Conceivable Turbulence Effects on Flame Velocity and Interpretation of the Experimental Test Data.

To understand the flame phenomena in a medium of turbulent flow it is necessary to proceed from the fact that the turbulent flow contains individual gas bodies which execute an irregular vibrational motion and with it enter the combustion zone. The approximate diameter of the gas bodies is given by the mixing length l, the approximate vibratory motion by the mean velocity fluctuation $|\overline{w'}|$. The transport processes amplified in the turbulent flow are identified by Prandtl's exchange quantity

$$\epsilon = l\,|\overline{w'}| \tag{67}$$

defined as a diffusion coefficient.

It is easy to visualize two turbulent flows 1 and 2 which, in macroscopic transport processes (that is such passing over the length of several diameters of turbulence bodies) are identically effective; hence

$$\epsilon_1 = \epsilon_2 \tag{68}$$

but at the same time can differ substantially in the hydrodynamic structure of the two flows. For condition (68) does not as yet indicate that it be necessary that

$$l_1 = l_2 \tag{69}$$

and

$$|\overline{w_1'}| = |\overline{w_2'}| \tag{70}$$

Merely the equality of the product $l_1 \left|\overline{w_1'}\right| = l_2 \left|\overline{w_2'}\right|$ is demanded. This indicates that the turbulence of a flow must be identified by two numerical values. Previously these were the Prandtl quantities l and ϵ; now they are the quantities l and $\left|\overline{w_1'}\right|$. It is therefore necessary to distinguish between a "coarse-body" turbulence with small velocity fluctuations and a "fine-body" turbulence with great velocity fluctuations. The effect of these two types of turbulence on the flame phenomena may be an entirely different one, although under practical test conditions both orders of magnitude of turbulence bodies are likely to be always present.

The effect of coarse-body turbulence with $l \gg \delta_L$[1] on a combustion zone can be explained as follows: Consider a pure laminar flow with a velocity profile as in figure 16(a). In this flow a perfectly smooth flame surface can exist at a place when the flow velocity $\overline{u}$ and the laminar flame velocity w_{fl} are exactly the same. Then visualize in the flow before entering the zone of the flame, the sudden appearance of a few turbulence bodies, so that for a moment the velocity profile shown in figure 16(b) is created. The flame surface at section a is now subjected to bulging in the flow direction similar to that on the Bunsen burner, where the laminar flame cone becomes so much more pointed as the flow velocity ($\overline{u} + u'$ in figure 16(b)) at point a exceeds the normal flame velocity w_{fl}. But in section b where the gas enters the flame surface with a velocity inferior to w_{fl}, it speeds against the gas (as in the flareback of a Bunsen burner). An inverted flame cone begins to form which grows continuously and thus speeds ever faster toward the gas flow. A stoppage or reversal of this flame motion occurs only with the sudden appearance of gas bodies at considerably greater flow velocity in section b, which must substantially exceed both $\overline{u}$ and $\overline{u} + u'$, as assmued on point a. Thus the coarse-body turbulence roughens the perfectly even flame surface in laminar flow and may leave it ruffled. But at the same time the effective flame surface apportioned to a definite flow cross section q in the turbulent flow becomes substantially greater than in laminar flow, as is readily apparent from a comparison of figures 16(b) and 16(a). In consequence the roughened or fringed flame surface can be kept stationary by a turbulent flow at a point in space only when at that point the mean flow velocity u, which, indeed must be equal to the turbulent flame velocity w_{ft}, referred to mean-flow cross section, is greater than the laminar flame velocity w_{fl}.

---

[1] δ_L is the experimentally determinable luminous zone thickness in the flame and indicates the thickness of the laminar combustion zone in order of magnitude.

Thus the coarse-body turbulence effects a rise of the flame velocity referred to flow cross section, even if the flame velocity in the individual microscopic flame surface elements, which for the most are diagonal to the principal flow direction, is entirely the same as in laminar flow; namely, w_{fl}.

This concludes the qualitative discussion of the effect of coarse-body turbulence. As to quantitative data it would entail the calculation of the extent to which the originally flat, laminar flame surface (cf. fig. 16) is enlarged by the sudden appearance of velocity fluctuations of the order u' in the flow and when the turbulence bodies have on an average the diameter l. Such a calculation would, of course, be almost impossible in the case of completely ruffled flame surface. But as long as the surface is only slightly wavy or roughened, such as is represented in figure 16(b), the flame surface could be approximated by a series of laminar Bunsen cones disposed side by side with variously directed cone tips, similar to the Meker burner where the entire surface of the flame consists of a series of side-by-side small Bunsen cones but all arranged in the same direction. Just as the enveloping surface of the flame cone on the Bunsen burner is in first approximation proportional to the mean flow velocity in the burner tube, so also it must be assumed that the surfaces of the individual positive and negative partial cones on the roughened flame surface are proportional to the velocity fluctuations $\pm u'$. Averaging over the entire flow cross section then would yield the proportionality

$$w_{ft} \sim |\overline{u'}| \tag{71}$$

or for constant turbulence-body diameters l, which in general depend only on the vessel's boundary (cf. fig. 13, which applies to turbulent tube flow):

$$w_{ft} \sim \epsilon \tag{72}$$

or finally, if $\frac{\epsilon}{\nu \mathrm{Re}}$ is approximately constant (as also holds true approximately for tube flow = nuclear flow in free jet, fig. 12):

$$w_{ft} \sim \mathrm{Re} \tag{73}$$

On these assumptions, about the occurrence of which in arbitrarily shaped reaction chambers nothing can, of course, be stated as yet, the turbulent flame velocity should be proportional to the Reynolds number Re.

What does the experiment say to this? Among the previously described experiments the coarse-body turbulence undoubtedly plays the

earliest part in the larger burner tubes II and III with their maximum mixing length computed at $l = 0.17$ and $l = 0.21$ millimeter for tube diameter $d = 2.18$ and 2.718 millimeters according to figure (13), while the thickness δ_L of the experimental luminous zone in laminar flow amounted only to about half, that is, 0.10 millimeter. Considering the maximum flame speeds w_{fmax} obtained for tubes II and III, they manifest no direct proportionality with Re, but still an approximate linear relationship (fig. 6)

$$w_{fmax} = A \times Re + B \tag{74}$$

The first term on the right-hand side possibly comprises the effect of the coarse-body turbulence. But in addition to that there is a second effect in term B, which also raises the flame speed and which carries particular weight at the small Reynolds numbers such as occur on the narrowest tube. Here, however, the turbulence bodies were already of the same order of magnitude as the thickness of the luminous zone δ_L; the maximum mixing length computed for tube diameter $d = 1.385$ millimeters was $l = 0.11$ millimeter according to figure (13). Hence it is very likely that the "fine-body" turbulence, at which the turbulence bodies are smaller than the thickness of the laminar δ_L, also played a part in these tests.

In analyzing the effect of this type of turbulence in the extreme limiting case $l \ll \delta_L$, no further roughening of flame surface may be expected, because the turbulence bodies have much too small a diameter for it. But a different effect must occur, namely, an amplification of every microscopic transport process in the flame surface, especially between the reaction zone and the preparatory zone. These transport processes, which, for example, effect the transfer of active particles or of heat from the reaction zone to the preparation zone, govern the flame speed very decisively, as is readily apparent from equation (15). According to it the flame speed is proportional to the square root of the transport quantity $\frac{\lambda_z}{\bar{c}_p \rho_a}$; hence

$$w_{fl} \sim \sqrt{\frac{\lambda_z}{\bar{c}_p \rho_a}} \tag{75}$$

Up to a factor departing little from unity this quantity $\frac{\lambda_z}{\bar{c}_p \rho_a}$ is, for gases, equal to the diffusion coefficient D and the kinematic viscosity ν. Observing, further, that in turbulent flow, according to equation (47), this transport quantity should be replaced by the Prandtl exchange quantity ϵ, it follows that in the extreme limiting case of

fine-body turbulence the ratio of turbulent to laminar flame speed is

$$\frac{w_{ft}}{w_{fl}} = \sqrt{\frac{\epsilon}{\nu}} \tag{76}$$

This formula is suitable for a mathematical check of the present study, since it not only presents a proportionality like equation (73) (which represents a limiting case of the coarse-body turbulence), but also a real, numerically assessable equation. In this instance the conditions are much better for the fine-body turbulence than for the coarse-body turbulence.

If this concept that for small burner tube diameters the fine-body turbulence also played an essential part along with the coarse-body turbulence, is correct, the maximum flame speeds $w_{f\,max}$ observed in the turbulent tests should not depart abnormally, in order of magnitude, from the flame speeds obtained by equation (76) and from the cited $\frac{\epsilon}{\nu}$ values in the free jet. This calculation is made easier by the fact that only the $\frac{\epsilon}{\nu}$ values of the free jet nucleus need to be taken into account, which by assumption were to agree with the values in pipe flow; for the greatest flame speeds in the present tests are undoubtedly assumed on the inside boundary of the turbulent flame zone, and this inner boundary definitely lies in all tests (except tests 52 and 45) within the nuclear zone of the free jet, as indicated by the dashed lines of figure 15. According to table 3 the ratio of the corresponding experimental inner cone surface lines to burner tube diameter, that is to say, $\frac{s}{d}$ was consistently much below 6. Hence an inside boundary of the turbulent combustion zone can be calculated by the differential equation

$$-\frac{d(h/R)}{d(r/R)} = \sqrt{\left(\frac{\bar{u}}{w_{fl}}\right)^2 \frac{\left(\frac{u_{max}}{\bar{u}}\right)^2 \left(\frac{u}{u_{max}}\right)^2}{\frac{\epsilon}{\nu}} - 1} \tag{77}$$

This equation is in perfect accord with equation (36) except for the difference that the $\frac{u}{u_{max}}$ values for turbulent flow replace the parabolic velocity distribution in laminar flow, and turbulent flame speed w_{fl} of equation (76) substitutes for the laminar flame speed w_{ft}. Equation (77) was graphically integrated for such $\frac{\bar{u}}{w_{fl}}$ values and those Reynolds numbers which approximately corresponded to the foregoing tests and for which the $\frac{\epsilon}{\nu}$ values could be taken directly from Nikuradse's report (reference 14). The numerical values of Re and $\frac{\bar{u}}{w_{fl}}$ employed are contained in table 9. The flame cones obtained by integrating (77) are reproduced in figure 17. As for the

evaluation of the experimental cones the length S of the enveloping surfaces and their center of gravity radius R' (cf. the figs. in the 4th and 5th cols. of table 9) were determined and from these data the flame speed $\bar{w}_{ft}$ averaged over the entire cone, was easily computed, because it is necessary that

$$w_{ft} = \frac{\bar{\bar{u}} R^2 \pi}{2\pi S R'} \tag{78}$$

or, when formed in ratio to the laminar flame speed:

$$\frac{\bar{w}_{ft}}{w_{fl}} = \frac{R^2}{2 R' S} \times \frac{\bar{\bar{u}}}{w_{fl}} \tag{79}$$

These data are reproduced in the next to the last column of table 9. They manifest no systematic motion with $\frac{\bar{\bar{u}}}{w_{fl}}$ at constant Reynolds numbers, so that averages are permissible (cf. last col., fig. 9)[1].

TABLE 9

Re	4×10^3		6.1×10^3		16.7×10^3		23.3×10^3	
$\sqrt{Re}$	63.2		78.0		129.1		152.7	
$\bar{\bar{u}}/w_{fl}$	10	15	10	15	20	40	20	40
S/R	3.925	5.925	3.265	4.910	4.310	8.59	3.61	7.41
R'/R	0.435	0.440	0.460	0.450	0.460	0.450	0.460	0.460
$\frac{w_{ft}}{w_{fl}} = \frac{R^2}{2S R'} \frac{\bar{\bar{u}}}{w_{fl}}$	2.93	2.88	3.33	3.39	5.04	5.17	6.03	5.87
Average for $\frac{\bar{w}_{ft}}{w_{fl}}$	2.90		3.36		5.10		5.95	

[1]The departure of the individual values $\frac{\bar{w}_{ft}}{w_{fl}}$ from the averages is even less than 2 percent, hence lies definitely within the range of errors of the employed method of graphical evaluation.

The turbulent flame speed thus computed therefore represents quantities computable from the entire surface of a flame cone located in the nuclear zone of the turbulent free jet and on which the flame speed of every flame surface element is increased in the ratio $\frac{\varepsilon}{\nu}$ relative to the laminar flame speed. Flame speed $\bar{w}_{ft}$ should agree then in order of magnitude with the experimental values of $\bar{w}_{fmax}$, if a substantial effect on the flame speed were due to the fine-body turbulence. And this actually appears to be the case: a comparison of the $\frac{\bar{w}_{ft}}{w_{fl}}$ values (dashed curve, fig. 6) with the experimental values $\frac{\bar{w}_{fmax}}{\bar{w}_{fmin}}$ shows the latter values to differ only by 30 percent from the former values; hence the order of magnitude of both quotients is definitely the same. Complete agreement is, of course, not to be expected; for the assumption of the extremely fine-body turbulence, where the turbulence bodies should be substantially inferior to the thickness of the laminar flame surface, is not fully complied with in the previously reported tests.

Figure 6(b) further shows that $\frac{\bar{w}_{ft}}{w_{fl}} \sim \sqrt{Re}$, as established in first approximation for the experimentally defined $\frac{\bar{w}_{fmax}}{\bar{w}_{fmin}}$ values at small Reynolds numbers. Admittedly, the factor of proportianality for both quotients is different, which proves again that another effect besides the fine-body turbulence, namely, the coarse-body turbulence, was involved in the tests. This is borne out by the fact that the form of computed inner boundary cones, illustrated in figure 17, does not exactly agree with the experimental, with their more bulging cones, as is evident from the flame photographs of figure 4.

Another unusual fact is that the observed $\frac{\bar{w}_{fmax}}{\bar{w}_{fmin}}$ values are smaller than the theoretically calculated $\frac{\bar{w}_{ft}}{w_{fl}}$ values. But this means that in transport processes over path lengths equal to or less than Prandtl's mixing length l, the exchange quantity ε is only partially effective. This finding may now seem perhaps trivial, but up to now the author has run across no experiment from which such could have been accurately deduced.

In conclusion, a few words about the outer demarcation of the turbulent flame zones. They extend in their upper part, especially on the largest of the employed tubes (III) far beyond the inner cross section of the tube. Here also the pressure difference before and after combustion may be involved as in the enlargement of the base of a

laminar Bunsen cone. However, some other factor besides this potential pressure effect must also have been effective, and this is very likely to be found in the marginal turbulence of the free jet. For the outer boundary surfaces of the turbulent flame zones lie to a great extent in the area of the marginal turbulence in the tests with tubes II and III. This is readily apparent when comparing the forms of these surfaces of demarcation with the cone-shape nuclear zone of the free jet of figure 15, and, further, when reflecting that the ratio $\frac{S}{d}$ for these boundary surfaces, on changing from tube I → tube II → tube III, moves continually nearer to the value 6 or even exceeds it (cf. table 3). The numeral 6, however, describes the ratio of enveloping surface to tube diameter (cf. fig. 15, also table 8) for the cone-shape nuclear zone of the turbulent free jet. In tests 52 and 45, where $\frac{S}{d}$ = 12.5 and 7.3, the cones extended especially far into the area of marginal turbulence.

Returning to the original question - that is, of the effect of the turbulence of a flow on the flame speed - the answer can be worded as follows: the turbulence always increases the flame speed referred to the average flow cross section, and in twofold manner: for coarse-turbulence bodies exceeding the laminar flame thickness, the flame surface is effectively enlarged, which is, by roughening or ultimate ruffling. For turbulence bodies smaller than the laminar flame thickness this phenomenon probably recedes in the background, though the flame speed increases by reason of the fact that all transport processes between reaction zone and preparatory zone in the flame surface are amplified, owing to the turbulent mixing motion. The effect of this fine-body turbulence can now be determined beforehand, but not that of the coarse-body turbulence. In the engine the coarse-body turbulence is most likely to assume the controlling part. Fine-body turbulence can be achieved only in flows issuing from very narrow tubes or slits of less than 1 millimeter, and such cross sections are avoided as much as possible for high-flow velocity because of the substantial flow resistances incidental to it.

Translation by J. Vanier,
National Advisory Committee
for Aeronautics.

REFERENCES

1. Nikuradse, J.: VDI – Forschungsheft, vol 3, no. 356, Sept.–Oct. 1932.

2. Tollmien, Walter: Calculation of Turbulent Expansion Processes. NACA TM No. 1085, 1945.

3. Prandtl–Tietjens: Hydro– und Aeromechanik, vol. 2, no. 24, 1931.

4. Mache, H.: Die Physik des Verbrennungserscheinungen, Leipzig, 1918.

5. Mallard, M. E.: Ann. d. Mines 7, 355, 1875.
Mallard, M. E., and Le Chatelier: Ann. d. Mines 4, 343, 1883.
Jouget, E: Comptes Rendus 156, 872, 1058, 1913.
Nusselt, W.: VDI–Zeitschrift vol. 59, 872, 1915.
Daniell, P. J.: Proc. Roy. Soc. London (A) 126, 393, 1930.
Lewis, B. and von Elbe, G.: Combustion Flames and Explosions of Gases. Cambridge, 1938, pp. 206ff.
Jost, W.: Explosions– und Verbrennungsvorgange in Gasen, Berlin, 1939, pp. 104ff.

6. Jost, W., and von Müffling, L.: Ztschr. physikal. Chem. A 181, 208, 1938.
Jost, W.: Ztschr. angew. Chem. 51, 687, 1938.

7. Damköhler, G.: Chem.–Ing. III, 1, 366ff. 1937.

8. Müller–Pouillet, Lehrbuch der Physik, Bd. III, 1, 859ff. 1926.

9. Chem. Taschenb. 3, 323, 1937.

10. Eucken, A.: Ztschr. techn. Physik 19, 517, 1938.

11. Schlichting, H.: Z.f.a.M.M. 13, 260, 1933.

12. Michelson: Über die normale Entzündungsgeschwindigkeit der Knall gasgemenge. Moscow, 1890.

13. Prandtl, L.: Z.f.a.M.M. 5, 136, 1925; Verh. d 2. Internat. Kongr. f. Tech. Mech., Zürich 1927; p. 62; Z.V.D.I. 77, 105, 1933.
Tollmien, Walter: Handb. d. Experimental–Physik IV, 1, pp. 309ff. 1931.

14. Betz, A.: Velocity and Pressure Distribution behind Bodies in an Air Current. NACA TM No. 268, 1927.
Förthmann, E.: Turbulent Jet Expansion. NACA TM No. 789, 1936.

Table 2.

Test No.	Flow velocity C_2H_2 N.T.P. cm³/s	Flow velocity O_2 N.T.P. cm³/s	Flow velocity $C_2H_2 + O_2 = G$ N.T.P. cm³/s	% C_2H_2	Δp mm H_2O	$\frac{G}{\Delta p}$	$\eta = \frac{\Delta p}{2{,}122 \cdot 10^{-6} \cdot G}$ g cm^{-1} s^{-1}	ϱ g/cm³	ν cm²/s
1	0,377	1,949	2,326	16,2	203,7	$1{,}14 \cdot 10^{-2}$	$1{,}86 \cdot 10^{-4}$	$1{,}43 \cdot 10^{-3}$	0,130
2	0,659	1,475	2,134	30,9	167,9	$1{,}27 \cdot 10^{-2}$	$1{,}67 \cdot 10^{-4}$	$1{,}52 \cdot 10^{-3}$	0,110
3	0,862	1,154	2,016	42,8	147,2	$1{,}37 \cdot 10^{-2}$	$1{,}55 \cdot 10^{-4}$	$1{,}59 \cdot 10^{-3}$	0,098
4	1,269	0,754	2,023	62,7	128,1	$1{,}58 \cdot 10^{-2}$	$1{,}34 \cdot 10^{-4}$	$1{,}70 \cdot 10^{-3}$	0,079
5	1,513	0,516	2,029	74,6	119,0	$1{,}71 \cdot 10^{-2}$	$1{,}24 \cdot 10^{-4}$	$1{,}77 \cdot 10^{-3}$	0,070
6	1,897	—	1,897	100,0	97,7	$1{,}94 \cdot 10^{-2}$	$1{,}09 \cdot 10^{-4}$	$1{,}92 \cdot 10^{-3}$	0,057
7	—	1,965	1,965	0	188,1	$1{,}04 \cdot 10^{-2}$	$(2{,}05 \cdot 10^{-4})$	$(1{,}34 \cdot 10^{-3})$	(0,153)
8	—	1,656	1,656	0	158,5	$1{,}04 \cdot 10^{-2}$	$(2{,}05 \cdot 10^{-4})$	$(1{,}34 \cdot 10^{-3})$	(0,153)
9	0,174	1,888	2,062	8,4	191,0	$1{,}08 \cdot 10^{-2}$	$1{,}96 \cdot 10^{-4}$	$1{,}39 \cdot 10^{-3}$	0,141
10	1,412	0,383	1,795	78,7	103,0	$1{,}74 \cdot 10^{-2}$	$1{,}22 \cdot 10^{-4}$	$1{,}80 \cdot 10^{-3}$	0,068
11	—	1,658	1,658	0	164,0	$1{,}01 \cdot 10^{-2}$	$(2{,}05 \cdot 10^{-4})$	$(1{,}34 \cdot 10^{-3})$	(0,153)
12	1,014	1,060	2,074	48,9	145,5	$1{,}42 \cdot 10^{-2}$	$1{,}49 \cdot 10^{-4}$	$1{,}62 \cdot 10^{-3}$	0,092
13	1,913	0,212	2,125	90,0	114,8	$1{,}84 \cdot 10^{-2}$	$1{,}15 \cdot 10^{-4}$	$1{,}86 \cdot 10^{-3}$	0,062
14	1,932	—	1,932	100	99,5	$1{,}94 \cdot 10^{-2}$	$1{,}09 \cdot 10^{-4}$	$1{,}92 \cdot 10^{-3}$	0,057
15	—	2,000	2,000	0	191,0	$1{,}04 \cdot 10^{-2}$	$(2{,}05 \cdot 10^{-4})$	$(1{,}34 \cdot 10^{-3})$	(0,153)

80*

Table 8

Nuclear flow

$\frac{r}{R}$	Re = $4{,}0 \cdot 10^3$			Re = $6{,}1 \cdot 10^3$			Re = $16{,}7 \cdot 10^3$			Re = $23{,}3 \cdot 10^3$		
	$\frac{l}{R}$	$\frac{\varepsilon}{\nu}$	$\sqrt{\frac{\varepsilon}{\nu}}$	$\frac{l}{R}$	$\frac{\varepsilon}{\nu}$	$\sqrt{\frac{\varepsilon}{\nu}}$	$\frac{l}{R}$	$\frac{\varepsilon}{\nu}$	$\sqrt{\frac{\varepsilon}{\nu}}$	$\frac{l}{R}$	$\frac{\varepsilon}{\nu}$	$\sqrt{\frac{\varepsilon}{\nu}}$
0,0	0,161	(2,0)	1,41	0,157	(2,0)	1,41	0,154	(2,0)	1,41	0,148	(2,0)	1,41
0,1	0,159	7,1	2,66	0,156	10,1	3,17	0,145	22,1	4,70	0,144	29,4	5,42
0,2	0,152	9,9	3,14	0,152	13,8	3,72	0,143	30,9	5,56	0,143	41,2	6,42
0,3	0,149	11,5	3,40	0,145	16,2	4,03	0,140	37,0	6,08	0,137	48,6	6,97
0,4	0,142	12,7	3,56	0,137	17,9	4,23	0,130	39,8	6,31	0,129	52,6	7,25
0,5	0,132	13,1	3,63	0,130	18,7	4,32	0,122	42,2	6,50	0,122	55,5	7,45
0,6	0,118	12,9	3,59	0,116	18,2	4,27	0,112	41,9	6,47	0,109	54,5	7,38
0,7	0,100	11,8	3,43	0,098	16,7	4,08	0,096	38,8	6,23	0,092	49,7	7,05
0,8	0,076	9,6	3,09	0,075	13,7	3,70	0,072	31,2	5,59	0,070	40,4	6,35
0,9	0,046	6,2	2,48	0,045	8,6	2,94	0,043	19,8	4,45	0,043	26,2	5,12
1,0	0,000	(1,0)	1,00	0,000	(1,0)	1,00	0,000	(1,0)	1,00	0,000	(1,0)	1,00

Marginal flow

$\frac{x}{R}$	For any Re			Re = $4{,}0 \cdot 10^3$		Re = $6{,}1 \cdot 10^3$		Re = $16{,}7 \cdot 10^3$		Re = $23{,}3 \cdot 10^3$	
	$\frac{b_1}{R}$	$\frac{b_a}{R}$	$\frac{b_1+b_a}{R}$	$\frac{l}{R}$	$\frac{\varepsilon}{\nu}$	$\sqrt{\frac{\varepsilon}{\nu}}$	$\frac{\varepsilon}{\nu}$	$\sqrt{\frac{\varepsilon}{\nu}}$	$\frac{\varepsilon}{\nu}$	$\sqrt{\frac{\varepsilon}{\nu}}$	$\frac{\varepsilon}{\nu}$	$\sqrt{\frac{\varepsilon}{\nu}}$
2	0,17	0,35	0,51	0,035	4,8	2,17	7,3	2,69	19,9	4,46	27,7	5,26
4	0,33	0,69	1,02	0,070	9,5	3,08	14,5	3,81	39,7	6,30	55,4	7,44
6	0,50	1,04	1,54	0,104	14,3	3,78	21,8	4,66	59,6	7,72	83,1	9,1
8	0,66	1,38	2,04	0,139	19,0	4,35	29,0	5,39	79,4	8,91	111	10,5
10	0,83	1,73	2,56	0,174	23,8	4,87	36,2	6,02	99	10	138	11,7
12,08	1,00	2,08	3,08	0,210	28,7	5,35	43,8	6,61	120	11	167	12,9

82*

Table 3

Test No.	Mole. weight of "propane"	Flow velocity cm³/s N.T.P. "Propane"	O_2	G = Propane + O_2	% Propane	ν cm²/s	Gaging of flame zone: Method*)	S-Cone surface line	R' = c.p. radius of S	F = cone surface cm²	Linear velocity $u = \frac{4G}{d^2\pi}$ cm/s	Flame velocity $\bar{w}_f = \frac{G}{F}$ cm/s	$\frac{\bar{w}_{f\,max}}{\bar{w}_{f\,min}}$	Reynolds number $Re = \frac{\bar{u}d}{\nu}$	$\sqrt{Re}$	Flame: Noisless	Flame: Whistles	$\frac{S}{d}$
Tube I: d = 0,1385 cm																		
11	45,7	2,12	21,54	23,66	8,96	0,140	K	0,465	0,040	0,117	1571	202,0		1555	39,4	yes	no	3,36
12		2,59	18,24	20,83	12,43	0,135	K	0,312	0,040	0,078	1383	266,0		1421	37,7	"	"	2,25
22	46,5	7,10	50,85	57,95	12,25	0,135	K	0,675	0,055	0,233	3860	248,5		3960	62,9	no	yes	4,87
25		5,08	38,20	43,28	11,72	0,136	K	0,665	0,041	0,171	2874	252,7		2933	54,1	"	"	4,80
49	46,17	2,628	13,05	15,68	16,75	0,129	Ph	0,245 0,243	0,037 0,032	0,057 0,0488	1042	275,0 321,0	1,17	1119	33,5	yes	no	1,77 1,75
50		3,64	10,33	13,97	26,02	0,117	Ph	0,360 0,350	0,0425 (0,031)	0,096 (0,068)	928	145,2 (205,0)	(1,41)	1098	33,1	"	"	2,60 2,53
51		7,90	29,55	37,45	21,10	0,123	Ph	0,565 0,538	0,050 0,038	0,177 0,128	2488	211,4 291,9	1,38	2800	52,9	no	yes	4,08 3,88
52		10,34	27,85	38,19	27,07	0,116	Ph	1,73	0,07	0,76	2537	50,2	?	3035	55,1	"	"	12,5
53	46,10	7,59	45,00	52,59	14,45	0,132	Ph	0,560 0,438	0,057 0,044	0,200 0,121	3500	262,0 434,7	1,66	3675	60,6	"	"	4,04 3,16
Tube II: d = 0,218 cm																		
28	46,34	0,656	14,68	15,34	4,28	0,147	K	0,49	0,069	0,213	411	72,2		612	24,7	yes	no	2,25
37	46,16	15,42	98,90	114,32	13,49	0,133	K	0,63	0,092	0,364	3065	314,1		5020	70,9	no	yes	2,89
42		15,40	99,40	114,80	13,41	0,133	Ph	0,66 0,435	0,10 0,07	0,414 0,191	3077	277,3 599,0	2,16	5036	71,0	"	"	3,03 2,00
43		15,60	90,75	106,35	14,67	0,132	Ph	0,643 0,420	0,097 0,066	0,392 0,174	2848	271,5 610,0	2,24	4711	68,6	"	"	2,95 1,93
44		16,33	49,25	65,58	24,90	0,118	Ph	0,715 0,49	0,095 0,072	0,427 0,222	1760	153,6 296,0	1,93	3250	57,0	"	"	3,28 2,25
45		17,80	41,15	58,95	30,15	0,112	Ph	1,59 1,03	0,108 0,072	1,08 0,466	1580	54,7 126,6	(2,31)	3075	55,5	"	"	7,29 4,72
46		6,33	15,15	21,48	29,46	0,113	Ph	0,67 0,648	0,067 0,055	0,282 0,224	576	76,2 96,0	1,26	1116	33,4	yes	no	3,07 2,97
47		6,56	17,23	23,79	27,57	0,115	Ph	0,578 0,57	0,065 0,052	0,256 0,186	638	100,8 128,0	1,27	1209	34,8	"	"	2,65 2,61
48		4,82	13,70	18,52	26,01	0,117	Ph	0,333 0,320	0,061 0,055	0,127 0,110	497	145,2 167,5	1,15	925	30,4	"	"	1,53 1,47
Tube III: d = 0,272 cm																		
54		85,5	231,8	317,3	26,95	0,116	Ph	2,050 1,193	0,194 0,110	2,50 0,825	5470	127,0 385,0	3,03	12850	113	no	yes	7,53 4,39
55		86,5	328,7	415,2	20,83	0,123	Ph	1,500 0,883	0,186 0,103	1,754 0,572	7150	237,0 725,9	3,06	15790	126	"	"	5,51 3,25
56		87,4	359,1	446,5	19,57	0,125	Ph	1,386 0,815	0,181 0,086	1,576 0,441	7690	283,0 1011	3,58	16700	129	"	"	5,10 3,00
57		89,3	374,3	463,6	19,26	0,126	Ph	1,413 0,800	0,180 0,088	1,598 0,443	7990	290,1 1046	3,61	17300	132	"	"	5,20 2,94

*) K = cathetometer measurements Ph = photographed

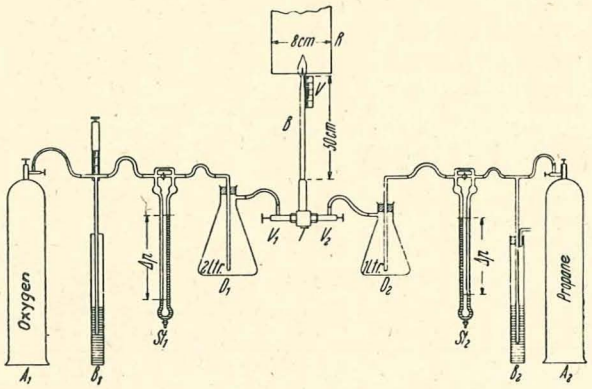

Figure 1.— Diagrammatic view of the test apparatus.

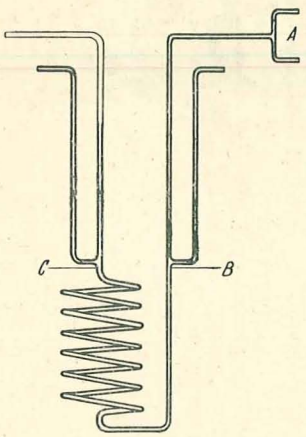

Figure 2.- Apparatus for measuring the viscosity of gas mixtures.

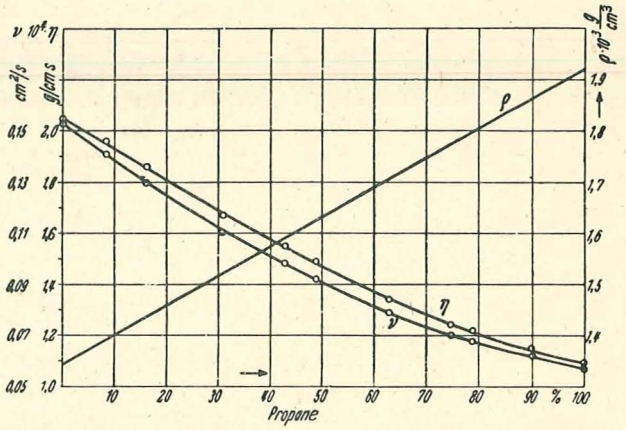

Figure 3.- Dynamic viscosity, kinematic viscosity and density for "propane" - oxygen mixture at 18 ± 1 °C.

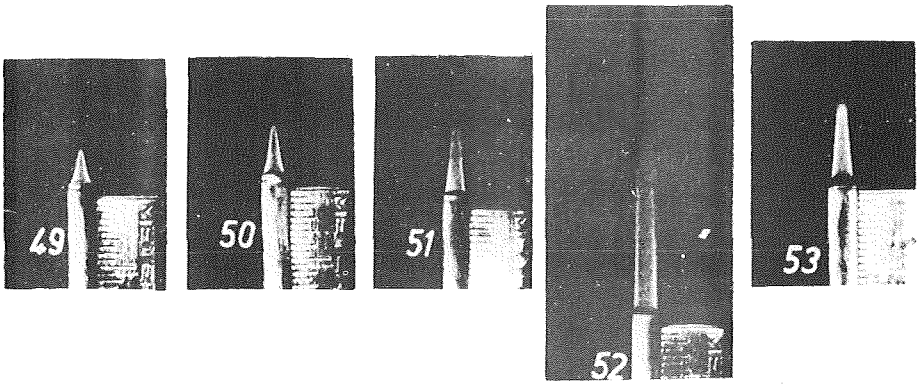

Tube I (d = 0,1385 cm)

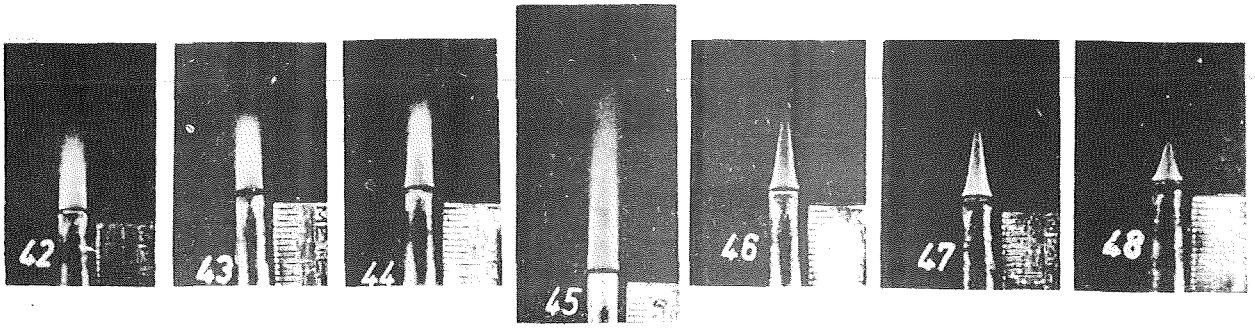

Tube II (d = 0.218 cm)

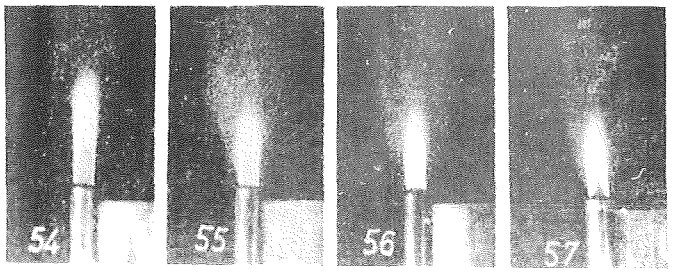

Tube III (d = 0.272 cm)

Figure 4.- Flame photographs, (tubes I, II and III).

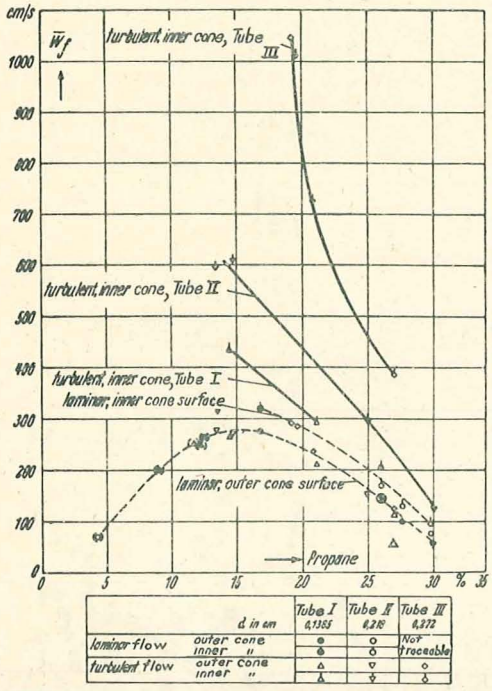

Figure 5.- Experimentally defined flame speeds $\overline{w}_f$ as function of the propane concentration.

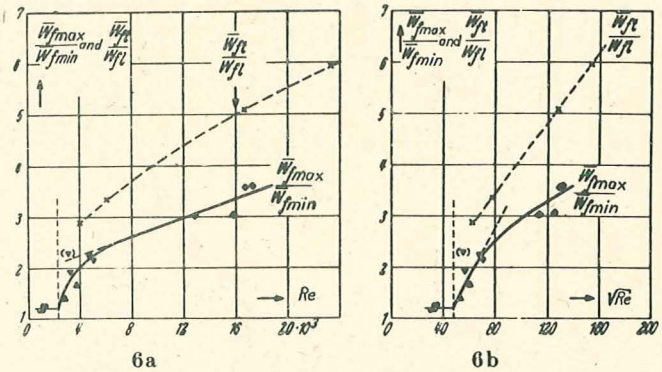

6a 6b

Figure 6.- Experimental values $\overline{w}_{f\,max}/\overline{w}_{f\,min}$ (solid curve) of the turbulent flame cone and comparison with the $\overline{w}_{ft}/w_{fl}$ values (dashed curves) theoretically computed for the case of extremely fine-body turbulence.

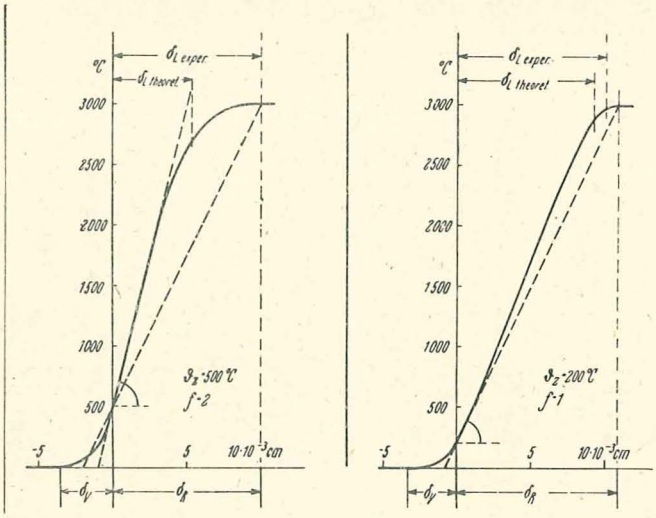

Figure 7.- Temperature variation in the laminar flame front at various hypothetical ignition temperatures ϑ_z and various f values.

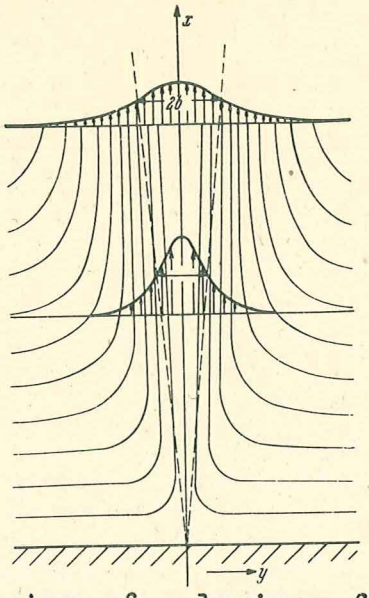

Figure 8.- Expansion of a laminar free jet according to Schlichting.

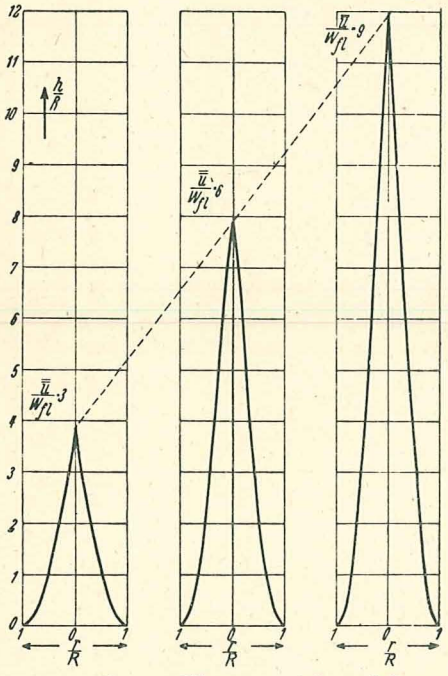

Figure 9.- Theoretically computed Bunsen cone in laminar flow.

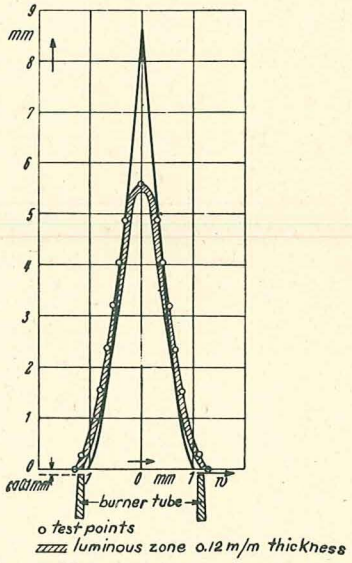

Figure 10.- Experimental Bunsen cone in laminar flow (test 47) compared with theoretically computed cone.

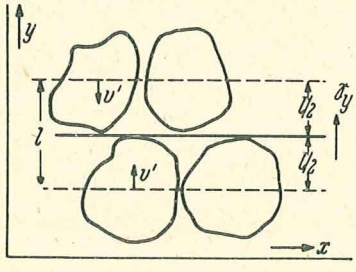

Figure 11.- Diagrammatic representation of a turbulent transport process according to the Prandtl mixing length theorem.

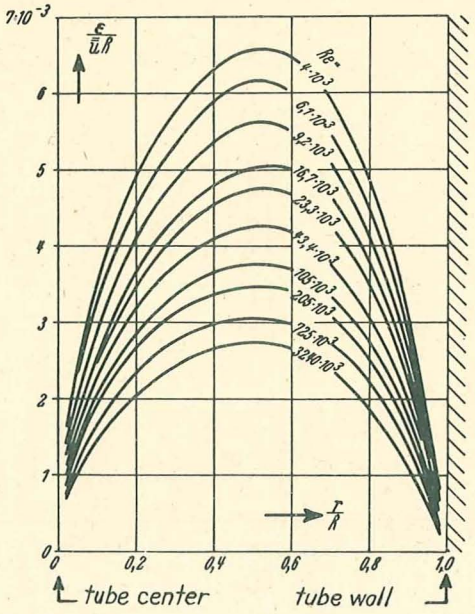

Figure 12.- Turbulent exchange quantity $\epsilon/\bar{u}R$ in tube flow as function of the relative distance from tube center line r/R at several Re in dimensionless representation.

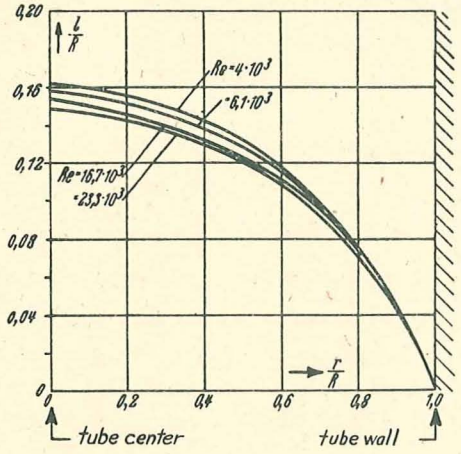

Figure 13.- Mixing length l/R in tube flow as function of the relative distance from tube center line r/R for several Re in dimensionless representation.

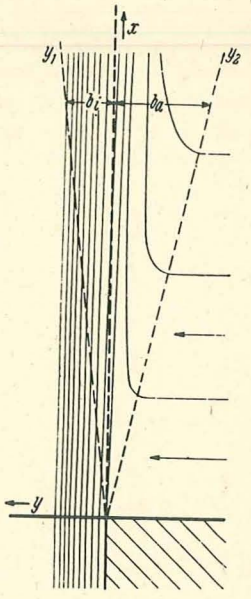

Figure 14.- Stream-line pattern of the turbulent marginal zone of a free jet (according to Tollmien).

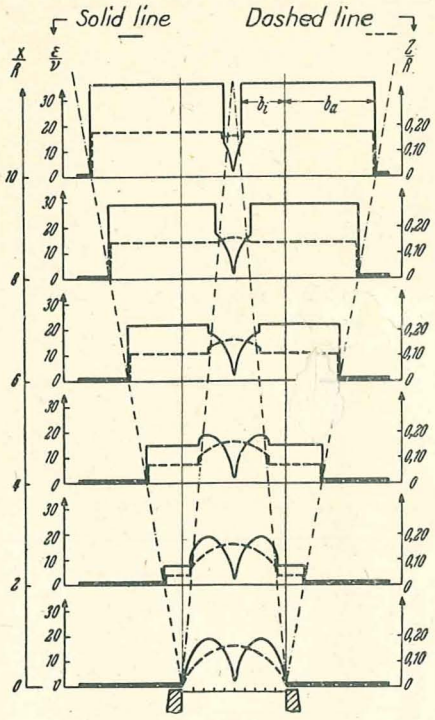

Figure 15.- Values of ϵ/ν and l/R for nuclear and marginal zone of turbulent free jet at various relative distances x/R from the tube orifice.

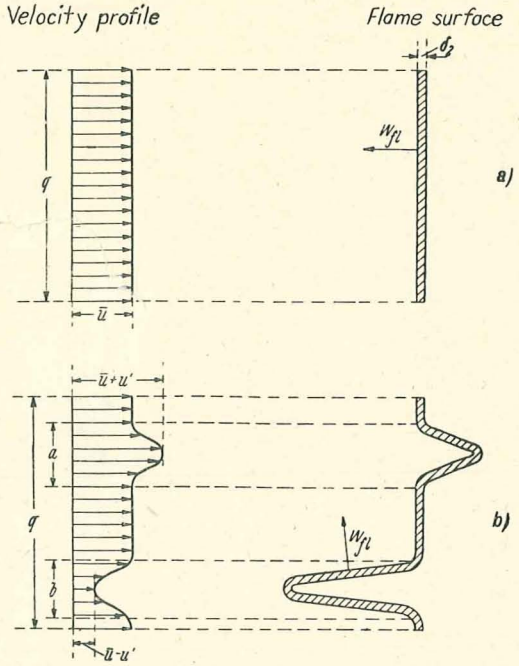

Figure 16.- Representation of the effect of coarse-body turbulence on an originally smooth flame surface.

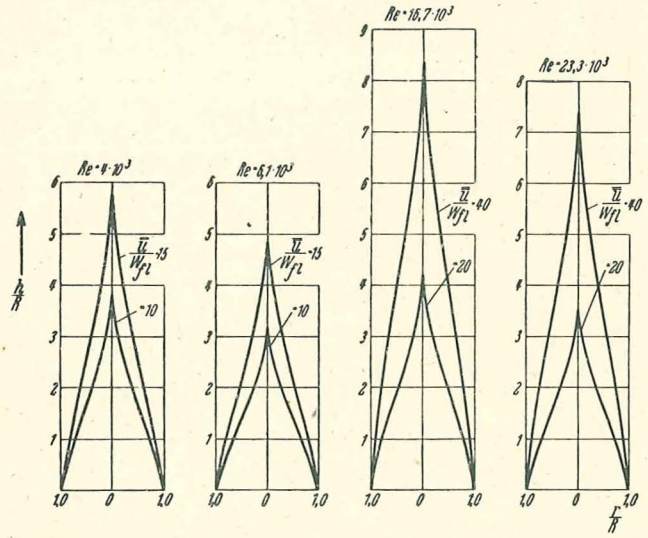

Figure 17.- Flame cones computed theoretically for the extreme limiting case of fine-body turbulence.